The American Journal of Pathology, Vol. 195, No. 12, December 2025

ELSEVIER

The American Journal of PATHOLOGY

ajp.amjpathol.org

TUMORIGENESIS AND NEOPLASTIC PROGRESSION

Interplay between Leptin and Stearoyl-CoA Desaturase 1 in Estrogen Receptor–Positive Breast Cancer Cells

Felice M. Accattatis,[*] Luca Gelsomino,[*†] Linda Manna,[*] Piercarlo Del Console,[*] Laura Bianchi,[‡] Alfonso Carleo,[‡] Rossana De Salvo,[‡] Lorenzo Arnaboldi,[§] Ludovica Baù,[§] Alberto Corsini,[§] Adele E. Leonetti,[*] Rocco Malivindi,[*¶] Marco Fiorillo,[*] Michael P. Lisanti,[‖**††] Cinzia Giordano,[*†¶] Daniela Bonofiglio,[*†] Sebastiano Andò,[*†] Stefania Catalano,[*†¶] and Ines Barone[*†]

From the Department of Pharmacy, Health and Nutritional Sciences and the Centro Sanitario,† University of Calabria, Arcavacata di Rende, Italy; the Laboratory of Functional Proteomics,‡ Department of Life Sciences, University of Siena, Siena, Italy; the Dipartimento di Scienze Farmacologiche e Biomolecolari "Rodolfo Paoletti,"§ Università degli Studi di Milano, Milan, Italy; the Clinical Laboratory Unit,¶ A.O. "Annunziata," Cosenza, Italy; Lunella Biotech, Inc.,‖ Ottawa, Ontario, Canada; the Royal Ottawa Hospital,** Institute of Mental Health Research, Ottawa, Ontario, Canada; and Translational Medicine,†† School of Science, Engineering and Environment, University of Salford, Greater Manchester, United Kingdom*

Accepted for publication August 14, 2025.

Address correspondence to Stefania Catalano, M.D., Department of Pharmacy, Health and Nutritional Sciences, University of Calabria, Via P. Bucci, Arcavacata di Rende (CS), 87036 Cosenza, Italy.
E-mail: stefania.catalano@unical.it.

Obesity, a global health challenge, contributes to various cancers, including breast cancer. Complex metabolic dysregulation marks the development of both breast cancer and obesity. Here, the interplay between the obesity-derived adipokine leptin (LEP) and stearoyl-CoA desaturase 1 (SCD), a critical enzyme in fatty acid (FA) metabolism, was explored. While Search Tool for the Retrieval of Interacting Genes/Proteins (STRING) database analysis reported a significant protein-protein interaction between LEP and SCD, functional processing of the differentially expressed genes in LEP-treated breast cancer cells revealed a critical involvement of SCD in the interactome of deregulated proteins. Kaplan-Meier analyses linked LEP/SCD expression to poorer recurrence-free survival in patients with estrogen receptor α luminal A-like breast cancer. Functional studies demonstrated that LEP up-regulated SCD expression in luminal A-like breast cancer cells through LEP receptor-mediated signaling. Lipidomic profiling showed that SCD inhibition using MF-438 reduced LEP-induced FA desaturation, characterized by a shift from saturated to monounsaturated FAs. SCD inhibition also abolished the LEP-mediated mitochondrial respiration and ATP production. Additionally, LEP-induced oncogenic features, including enhanced growth and motility, were counteracted by pharmacologic/genetic SCD blockade, confirming SCD's role in leptin's protumorigenic effects. This study highlights the LEP-SCD axis as a driver of metabolic/functional alterations in estrogen receptor α–positive breast cancer, providing insights into the obesity–breast cancer link and identifying potential therapeutic targets (ie, SCD) to counter obesity-driven cancer progression. *(Am J Pathol 2025, 195: 2492–2511; https://doi.org/10.1016/j.ajpath.2025.08.009)*

Supported by Projects of Relevant National Interest (PRIN) 2022–European Union's NextGenerationEU initiative under the Italian Ministry of University and Research–M4C2-I1.1 number 202239N8PR, Unique Project Code (CUP) H53D23006360006, and PRIN National Recovery and Resilience Plan (PNRR) 2022–European Union's NextGenerationEU initiative under the Italian Ministry of University and Research as part of the PNRR–M4C2-I1.1 number P2022YAKJY, CUP H53D23010120001 (I.B.); PRIN 2022, European Union's NextGenerationEU initiative under the Italian Ministry of University and Research–M4C2-I1.1 number 2022AA4FTJ, CUP H53D23006420006 (C.G.); Italian Association for Cancer Research (AIRC) investigator grant 2024 number 30782 (S.C.); AIRC investigator grant 2021 number 26246 (S.A.); and PRIN PNRR 2022–European NextGenerationEU initiative under the Italian Ministry of University and Research as part of the PNRR–M4C2-I1.1 number P2022FK2J8, CUP H53D23010420001 (L. G.).

F.M.A. and L.G. are joint first authors.

https://doi.org/10.1016/j.ajpath.2025.08.009

Breast carcinoma is the most commonly diagnosed malignant neoplasm in the female population worldwide and is the most frequent cause of death from neoplastic disease.[1] A comprehensive overview of breast tumorigenesis suggests that this process is influenced not only by intrinsic properties of the tumor cells, but it is also tightly dependent on the surrounding microenvironmental factors and on the host characteristics.[2] Indeed, several studies have now recognized obesity, a metabolic disorder characterized by an abnormal accumulation of body fat, as a heavyweight player able to drive development and progression of breast cancer, especially concerning postmenopausal status and estrogen receptor (ER) α− and progesterone receptor−positive tumor subtypes.[3]

Obesity is associated with an expanded, metabolically active and reprogrammed adipose tissue that induces altered secretion of several bioactive molecules.[4–6] These local changes cooperate with systemic obesity-associated alterations to impact cancer through direct effects on neoplastic epithelial cells or through indirect effects mediated by adipocytes within the tumor microenvironment, then deeply affecting tumor progression, and patient's outcome.[4–6] One of the most important features in obesity−breast cancer link is represented by the imbalance in adipokine production and, in this context, leptin (LEP) plays a central role. LEP, a 16-kDa neuroendocrine peptide hormone, beyond being a key regulator of food intake and energy homeostasis, is able to orchestrate different pathways involved in breast tumorogenesis. LEP can influence proliferation, growth, invasion, and metastasis by binding to its receptor (ObR) expressed in breast carcinoma cells.[7,8] Additionally, LEP is a significant factor in metabolism, particularly in lipid metabolism, because it is involved in various pathophysiological mechanisms that affect lipid absorption, storage, and utilization.[9–11]

The profound reprogramming of cellular metabolism, a fundamental characteristic of oncogenic transformation, is now considered a hallmark of cancer.[12] The main metabolic characteristics may include the following: i) aerobic glycolysis, designated as the Warburg effect, a major metabolic feature shared by most cancer types; ii) dependence on glutamine, which replenishes the tricarboxylic acid cycle; iii) consumption of acetate and folate, to support lipid and nucleotide biosynthesis; and iv) increased fatty acid (FA) biosynthesis, because neoplastic cells require large amounts of lipids and cholesterol. Within this broad spectrum of changes, the enzyme stearoyl-CoA desaturase (SCD) plays an important role as activator of *de novo* lipogenesis and cholesterol biosynthesis.[13] In humans, two distinct isoforms of SCD have been identified: SCD1 (hereafter referred to as SCD), the predominant and ubiquitously expressed isoform, and SCD5.[14] Mainly, SCD is an enzyme that catalyzes the conversion of saturated FAs (SFAs) palmitic and stearic to Δ9-monounsaturated [monounsaturated fatty acid (MUFA)] palmitoleic and oleic FAs.[15] These four specific FAs are major components of all principal lipid classes, including phospholipids, diacylglycerols, triglycerides (TGs), cholesteryl esters (CEs), and free FAs. They serve as basic components of biological membranes, energy sources, and signaling molecules crucial for cellular communication.[16] SCD overexpression is associated with poor prognosis in different cancer types,[17–21] and strong experimental evidence indicates that increased expression and activity of SCD are critical in malignant breast behaviors.[22–25] SCD can modulate cancer development and growth through various signaling pathways, some of which overlap with LEP's transduction pathways, including epidermal growth factor/epidermal growth factor receptor, endoplasmic reticulum stress/unfolded protein response, phosphatidylinositol 3-kinase/AKT, cyclin-dependent kinases 4 to 6 (cyclinD1/CDK4-6), extracellular signal-related kinases 1/2−mitogen-activated protein kinase, phosphatase and tensin homolog/AKT, and AKT/glycogen synthase kinase 3β/β−catenin.[16] Moreover, 17β-estradiol, which is well known to cross-talk with LEP signaling,[26–30] was previously described inducing cell proliferation and SCD expression via sterol regulatory element binding protein 1 (SREBP1) ERα-positive MCF-7 and T47D breast cancer cells but not in nontumorigenic epithelial cell line MCF-10A cells. Because tamoxifen reverted this effect, SCD was proposed as a therapeutic target in ERα-positive breast cancer.[31] An interplay between LEP and SCD has been suggested in liver[32] and neuronal cells[33] during obesity. In hepatocyte carcinoma cells, which expressed LEP receptor (ObR),[34] it was demonstrated that LEP reduced SCD gene transcription,[35] whereas LEP silencing resulted in SCD down-regulation through SREBP1 inhibition in nasopharyngeal carcinoma cells.[36]

Here, it has been investigated the potential functional interaction between LEP and the SCD enzyme in ERα-positive breast cancer cells and whether this mechanism could be significant in mediating the protumor effects mediated by LEP.

Materials and Methods

Antibodies and Reagents

Antibodies against SCD (sc-58420), SREBP-1 (sc-13551), glyceraldehyde-3-phosphate dehydrogenase (sc-47724), and β-actin (sc-69879) were acquired from Santa Cruz Biotechnology (Dallas, TX). Recombinant Human Leptin Lyophilized (PHP0013) was obtained from Thermo Fisher Scientific (Waltham, MA). The SCD inhibitor MF-438 (921605-87-0) was acquired from Sigma-Aldrich (Milan, Italy). Oligomycin A (75351) was acquired from Merck (Milan, Italy). Bedaquiline (TMC-207) was purchased from AdooQ Bioscence (Irvine, CA).

Cell Cultures

Human MCF-7, T47D, MDA-MB-231, and SKBR-3 breast cancer cells were purchased from ATCC (Manassas, VA) and cultured following supplier's instruction. MCF-7 and MDA-MB-231 cells were cultured in Dulbecco's modified Eagle's medium (DMEM) F12 medium (Thermo Fisher Scientific) containing 10% fetal bovine serum (FBS), 1% L-glutamine, and 1% penicillin-streptomycin (Thermo Fisher Scientific) at 37°C with 5% CO_2 air. T47D and SKBR-3 cells were cultured in RPMI 1640 medium (Thermo Fisher Scientific), supplemented with 10% FBS and 1% penicillin-streptomycin at 37°C in humidified 5% CO_2 air. Cells were authenticated every 6 months at the Sequencing Core and regularly tested for *Mycoplasma* negativity (MycoAlert; Lonza, Basel, Switzerland). The cell lines were used within 3 months of culture and before the 20th passage.

Lentiviral Transfection

The establishment of a stable MCF-7 cell line has been achieved by using control shRNA lentiviral particles (TR30021V; OriGene Technologies, Rockville, MD) and SCD shRNA lentiviral particles (TL309631V; OriGene Technologies) following manufacturer's instructions. Cells were selected using 1 μg/mL puromycin over time to eliminate uninfected cells. SCD protein expression in stable clones was evaluated by immunoblotting analysis. Previously generated stable control sh and ObR sh MCF-7 cell lines, by using control shRNA lentiviral particles-A (number sc-108080; Santa Cruz Biotechnology) and ObR shRNA (h) lentiviral particles (number sc-36115-V; Santa Cruz Biotechnology),[37] were also used.

Interactomics Prediction of SCD Involvement in MCF-7 Response to Leptin

Count data from previous work [accession number in European Bioinformatics Institute (EBI) ArrayExpress database (E-MTAB-3641); *https://www.ebi.ac.uk/biostudies/ArrayExpress/studies/E-MTAB-3641?query=E-MTAB-3641*,[38] last accessed December 15, 2024], which investigated LEP effects on the transcriptome of MCF-7 cells, were log2 transformed, background corrected, and quantile normalized by DeSeq2 Rpackage version 4.4.[39] Transcripts with low expression levels (exhibiting a count per million value lower than 1) were excluded from the analysis. After a preliminary comparison performed, including all the investigated experimental conditions, the analysis was narrowed on the comparison between LEP-treated and control cells using limma R package version 3.62.2 (*https://www.r-project.org*,[40] last accessed December 20, 2024). Transcripts presenting an absolute $\log_2$ fold change higher than 1 and a P value < 0.002, as determined by the Benjamini-Hochberg correction for false discovery rate, were designated as differentially expressed genes (DEGs) in the LEP-treated versus control cell comparison and selected for the interactomics analysis. Enrichment analysis of protein-coding DEGs (presenting an unambiguous UniProt identifier) were obtained through enrichR R package version 3.2 (*https://www.r-project.org*,[41] last accessed December 20, 2024). Only the enriched terms having at least five genes of interest and a P value < 0.05 at Benjamini-Hochberg test of the false discovery rate were considered as significant.

The MetaCore version 23.3 network building tool (Clarivate Analytics, Boston, MA) was applied to functionally correlate DEG-coded proteins by using the direct interaction algorithm and according to the MetaCore curated database of protein-protein interactions (PPIs). Only proteins with direct functional correlations entered into the direct interaction network (DIN), which represents the interactomic core of the investigated processes. MetaCore networks are visualized as nodes (proteins) and edges (interactions) and named after their top five hubs. These, being the seed nodes cross-linked to the higher number of net factors, they are recognized as critical biomarkers with key roles in defining the system biochemical properties and for clinical applications, as previously demonstrated.[42–44]

PPI Network Construction and Enrichment Analysis

The PPI network of the candidate LEP and SCD proteins was generated using the Search Tool for the Retrieval of Interacting Genes/Proteins (STRING) version 12.0 database (*https://string-db.org/cgi/input?sessionId=bp7GGoXn66Fl&input_page_show_search=on*, last accessed February 10, 2025). The confidence of the interaction was set to medium confidence (0.4).

Survival Kaplan-Meier Analysis

Kaplan-Meier plots were generated by using the Kaplan-Meier plotter online tool (*https://kmplot.com/analysis*, last accessed January 4, 2025), to evaluate the correlation of *LEP* and *SCD* mean expression levels with recurrence-free survival in all breast cancer subtypes and in patients classified, according to the StGallen classification, into luminal A, luminal B, human epidermal growth factor receptor 2 $(HER2)^+$, and basal subtypes, with auto select best cutoff, and the JeSet best probe set, in The Cancer Genome Atlas, Gene Expression Omnibus, and Metabric data sets.[45] Hazard ratios with 95% CIs and log-rank P values were calculated and plotted in R version 3.0.1, as previously described.[46]

Leptin Treatment

Cells were seeded in DMEM F12 medium (MCF-7) or RPMI 1640 medium (T-47D) without phenol red, supplemented with 5% or 10% FBS, respectively. After 24

hours, the medium was replaced with DMEM F12 or RPMI 1640 medium containing charcoal stripped FBS. Recombinant Human Leptin Lyophilized was administered at a final concentration of 500 ng/mL, with the exact treatment duration varying depending on the specific experimental protocol. For lipidomic analyses, cells were seeded in DMEM F12 without phenol red and supplemented with 5% FBS. After 24 hours, the medium was replaced with DMEM F12 supplemented with charcoal stripped FBS. LEP treatment was performed for 3 days, and for experiments extending to 6 days, medium containing LEP was refreshed on day 3 to maintain consistent exposure. Leptin concentrations applied in *in vitro* experiments to induce proliferation might closely mimic the local paracrine environment present within breast adipose tissue, a major component of the breast cancer microenvironment.

SREBP1 siRNA Silencing

Cells were transfected with SREBP1 (SREBF1) Human siRNA Oligo Duplex (locus identifier 6720; OriGene Technologies) and with Trilencer-27 Universal scrambled negative control siRNA duplex (SKU SR30004; OriGene Technologies), used as a negative control, using Lipofectamine RNAi/MAX reagent (13778075; Thermo Fisher Scientific), according to the manual instructions. Specifically, 35×10^4 MCF-7 cells were transfected with 10 nmol/L of both validated SREBP1 (SREBF1) Human siRNA Oligo Duplex or Trilencer-27 Universal scrambled negative control siRNA duplex in 6-well plates. On the following day, MCF-7 cells were treated as indicated for a further 24 hours.

Immunoblot Analysis

Cells were lysed in radioimmunoprecipitation assay buffer (50 mmol/L Tris-HCl, 150 mmol/L NaCl, 1% Nonidet P-40, 0.5% sodium deoxycholate, 2 mmol/L sodium fluoride, 2 mmol/L EDTA, and 0.1% SDS) containing a mixture of protease inhibitors (aprotinin, phenylmethylsulfonyl fluoride, and sodium orthovanadate). Equal amounts of cells extracts were resolved on 11% SDS-polyacrylamide gel, as described.[47] Odyssey FC and Image Studio Lite software version 5.2.5 (Licor, Lincoln, NE) were used to acquire and quantify the band of interest.

Quantitative Real-Time RT-PCR Assay

Total RNA from cells was extracted by using the TRIzol reagent (Thermo Fisher Scientific). A NanoDrop-1000 spectrophotometer (Thermo Fisher Scientific) was used to evaluate RNA concentration and quality. Two micrograms of total RNA was reverse transcribed with the RETROscript Kit (Applied Biosystems, Monza, Italy). Gene expression has been analyzed by real-time RT-PCR using an SYBR Green Universal PCR Master Mix (Bio-Rad, Hercules, CA) in an iCycler iQ Detection System (Bio-Rad). The relative gene expression levels were assessed and calculated as previously described.[47] Each sample was normalized on *18S* mRNA expression. Primers are listed in Table 1.

Immunofluorescence

Cells were fixed using 4% paraformaldehyde, and permeabilized with phosphate-buffered saline containing 0.2% Triton X-100. Blocking was performed with 5% bovine serum albumin for 1 hour at room temperature. The cells were then incubated overnight at 4°C with an anti-ObR primary antibody (sc-8391; dilution 1:100), followed by incubation with fluorescein isothiocyanate—conjugated secondary antibody (F3008; Sigma-Aldrich) for 30 minutes at room temperature. A primary IgG antibody was used as negative control. Nuclear staining was performed using DAPI (Sigma-Aldrich). Fluorescent images were captured using an Olympus BX51 microscope (Tokyo, Japan), with a 100× objective.

Immunohistochemistry Analysis of MCF-7 Breast Tumor Xenografts

In accordance with the 3Rs as reuse, in which all animals were maintained and managed in accordance with the recommendations of the *Guide for the Care and Use of Laboratory Animals*,[48] formalin-fixed, paraffin-embedded tissues from previous female 45-day—old athymic nude

Table 1 Oligonucleotide Primers Used in This Study

Gene name	Gene symbol	Species	Forward or reverse	Primer sequences
Leptin receptor	*ObR long*	Human	Forward	5′-GATAGAGGCCCAGGCATTTTTTA-3′
Long isoform			Reverse	5′- CACCACTCTCTCTCTTTTTGATTGA-3′
Leptin receptor	*ObR short*	Human	Forward	5′-ATTGTGCCAGTAATTATTTCCTCTTCC-3′
Short isoform			Reverse	5′-CCACCATATGTTAACTCTCAGAAGTTCAA-3′
Stearoyl-CoA desaturase 1	*SCD-1*	Human	Forward	5′-TGCCCACCACAAGTTTTCAG-3′
			Reverse	5′-CATCAGCAAGCCAGGTTTGT-3′
18s rRNA	*18s*	Human	Forward	5′-CGGCGACGACCCATTCGAAC-3′
			Reverse	5′-GAATCGAACCCTGATTCCCCGTC-3′

mice injected orthotopically with control sh and ObR sh MCF-7 clones were used.[37] Incubations with primary SCD antibody were performed at room temperature overnight in a humidified chamber. Normal goat serum was used as blocking agent. Biotinylated horse anti-mouse/rabbit (1:100) was used as the secondary antibody and revealed with a Vectastain ABC Kit Elite (catalog number PK-6200; Vector Laboratories, Burlingame, CA) and a Peroxidase Substrate Kit DAB (catalog number SK-4100; Vector Laboratories). All stained slides were visualized using an Olympus BX41 microscope, and the images were taken with CSV version 1.15 software (Olympus, Evident Europe GmbH, Hamburg, Germany), using a CAM XC-30 for image acquisition.

Lipidomics

After harvesting, treated and untreated cell samples were extracted three times by a 2:1 mix of $CHCl_3$/CH_3OH, KCl 0.05%, and butylated hydroxytoluene as antioxidant. Proper internal standards (stigmasterol, cholesteryl heptadecanoate, and triheptadecanoin) were added to the extraction mixture to quantify the mass of the lipid subclasses (free, esterified cholesterol, and triglycerides, respectively). While total fatty acid (qualitative) profile analysis was directly performed on aliquots of lipid extract, lipid subclasses were first separated onto thin layer chromatography silica gel 60 plates (Merck, Milan, Italy). After development in hexane/diethylether/acetic acid (80:20:1) and dichlorofluorescein staining, lipid subclasses were identified by comparison of their spots with those of standards and scraped off from the silica. Before gas-liquid chromatography analysis, aliquots of whole lipid extract or of silica gel containing the lipid subclasses were derivatized by methanolic HCl 3N for 30 to 120 minutes at 80°C; the obtained methylated FAs were extracted with hexane/water and injected in a gas-liquid chromatograph (DANI 1000; DANI, Milan, Italy) equipped with a flame-ionization detector, hydrogen as gas carrier, and an HTA autosampler (HTA Instruments, Brescia, Italy). For fatty acid profile of total lipid extract, cholesteryl esters, and triglycerides, a MEGA-5 capillary column (0.25-mm internal diameter, 30-m length; MEGA Columns, Legnano, Italy) was used, and the oven temperature was programmed as follows: 150°C to 190°C at 8°C/minute; from 190°C to 210°C at 4°C/minute and to 320°C at 12°C/minute, hold for 6 minutes, for a total run of 25.5 minutes. The identification of each fatty acid was achieved by comparing the retention times of each peak with those of a standardized mixture of methylated fatty acids (FAME MIX 37; Sigma-Aldrich). The relative amount of each fatty acid was calculated by the Clarity Software version 8.7 (Clarity, Prague, Czech Republic), by summing the areas under the curve of each peak and calculating the relative percentages.[49]

Seahorse XFe96 Metabolic Flux Analysis

The Mito Stress Test was used to evaluate the cellular metabolic profile by measuring real-time oxygen consumption rates (OCRs) using the Seahorse Extracellular Flux Analyzer (XFe-96; Agilent Technologies, North Billerica, MA). Briefly, breast cancer cells (10^4 cells/well) were seeded in 150 μL of culture medium into XFe-96 cell culture plates and allowed to adhere for 24 hours. The following day, cells were treated as indicated. After washing with prewarmed XF assay medium, supplemented with 10 mmol/L glucose, 1 mmol/L pyruvate, and 2 mmol/L L-glutamine, cells were incubated at 37°C in a non-CO_2 incubator for 1 hour. For mitochondrial respiration assessments, sequential injections of 1 μmol/L oligomycin (an ATP synthase inhibitor), 1 μmol/L carbonyl cyanide-p-trifluoromethoxyphenylhydrazone (FCCP; a mitochondrial uncoupler), and 0.5 μmol/L rotenone/antimycin A mix (inhibitors of complex I and III of the electron transport chain) were performed to calculate specific respiratory parameters. All experiments were performed independently in duplicate, with each condition tested in quintuplicate. Data were normalized to cell mass as determined by the sulforhodamine B assay.

Sulforhodamine B Assay

At the end of the seahorse experiment, 10% trichloroacetic acid was added to the cells for 1 hour at 4°C, and after that, sulforhodamine B dye (Acid Red 52; Sigma-Aldrich) was used for 30 minutes at room temperature. Cells were then washed twice with 1% acetic acid and air dried for at least 3 hours. Finally, the cells were resuspended in 10 mmol/L Tris, pH 8.8, solution, and the absorbance was measured at a wavelength of 565 nm (Multiskan SkyHigh; Thermo Fisher Scientific).

Cellular ATP Quantification

Intracellular ATP levels were assessed using an ATP Assay Kit (number ab83355; Abcam, Cambridge, UK) and following the manufacturer's protocol. Briefly, 3.5×10^5 breast cancer cells were plated in medium for 24 hours and then treated as indicated for a further 48 hours. OD (570 nm) was measured using a microplate reader (Multiskan SkyHigh).

Wound Healing Assay

Cells were plated (10^5/well) in complete medium in 6-well plates. Confluent monolayers were starved with their respective phenol red−free culture media supplemented with 3% charcoal stripped FBS for 24 hours and, at optimal confluence, a scratch was performed using a pipette tip. Cells were then treated as indicated for 24 hours. Afterwards cells were fixed and stained with Coomassie Brilliant

Blue. Images were taken at ×10magnification using an Olympus BX51 microscope, and the percentage of wound closure was analyzed by using ImageJ software version 1.52a (NIH, Bethesda, MD; *https://imagej.net/ij*), quantifying the wound opening area.

Anchorage-Independent Soft Agar Growth Assays

Anchorage-independent growth assays were conducted as previously described.[50] Data represent three independent experiments performed in triplicate.

Statistical Analysis

Statistical analysis was performed with analysis of variance using GraphPad Prism 8 (GraphPad Software, Inc., San Diego, CA) and reported as the means ± SEM.

Results

Leptin and SCD Interplay in ERα-Positive Luminal-Like Breast Cancer Cells

To explore potential interactions between LEP and SCD, the STRING database was used (*https://string-db.org*, last accessed February 10, 2025). The analysis yielded a network comprising seven nodes, encompassing a range of proteins associated with breast cancer biology and lipid metabolism, including CIDEC,[51–53] ELOVL6,[54–56] GPAM,[57,58] and ADIPOR2.[59–63] Noteworthy, LEP and SCD exhibited the highest number of connections, each having six connections (PPI enrichment $P = 0.000124$) (Figure 1A). Then, the clinical significance of both *LEP* and *SCD* gene expression in human breast cancers was studied by using Kaplan-Meier plots. Elevated expression levels of both *LEP* and *SCD* were found to be correlated with poorer recurrence-free survival in patients with breast cancer across multiple independent data sets (Figure 1B). A further analysis of the co-expression of *LEP* and *SCD* in different breast cancer subtypes, classified according to the St. Gallen criteria, showed that high expression of both genes significantly correlates with a poorer recurrence-free survival exclusively in patients with luminal A breast cancer (Figure 1C). On the basis of these findings, the role of LEP and SCD was further investigated in ERα-positive luminal A-like breast cancer cell lines.

Thus, to assess whether LEP may affect SCD gene and protein expression, the present study used two well-known ERα-positive luminal A-like breast cancer cell lines (namely, MCF-7 and T-47D). Cells were treated with LEP (500 ng/mL) for 6, 12, and 24 hours to investigate, by quantitative real-time RT-PCR, *SCD* expression, and for 12 and 24 hours for immunoblotting detection of SCD protein abundance. Both cell lines showed an increase in *SCD* gene expression, reaching the zenith at 12 hours in MCF-7 breast cancer cells (Figure 2A), and at 6 hours in T47D breast cancer cells (Figure 2B). Concerning protein expression, the maximal expression of SCD was reached 12 hours after LEP administration in both cell lines (Figure 2, C and D). Moreover, no leptin-mediated up-regulatory effects in SCD protein expression were detected in triple-negative basal-like MDA-MB-231 and in ERα-negative/HER2-overexpressing SKBR-3 breast cancer cell lines, suggesting that the effect of leptin on SCD expression is depending on the specific cellular background (Figure 2, E and F). To demonstrate the direct involvement of LEP/ObR-mediated signaling in the observed SCD up-regulation, the present study used MCF-7 cells stably silenced for ObR using lentiviral delivered short hairpin RNA (ObR sh). Ob mRNA and protein levels, as measured by quantitative real-time RT-PCR and immunofluorescence, were significantly down-regulated in ObR sh clones compared with cells stably transfected with a vector shRNA (Control sh) (Supplemental Figure S1). As expected, LEP treatment induced a significant increase of *SCD* gene expression in Control sh MCF-7 cells, whereas LEP effects were reversed in ObR sh breast cancer cells (Figure 2G). Results were also confirmed by immunoblotting analysis (Figure 2H), although at 12 hours, a slight increase in SCD expression was still observed, which may reflect a transient or partial regulation by alternative pathways. By using the same experimental model, a significant reduction in tumor volume has been previously demonstrated in mice injected with ObR sh cell lines compared with the control counterpart, concomitant with a decrease in Ki-67 expression and the mitotic index.[37] Thus, to further explore the link between LEP and SCD, SCD expression has been evaluated in formalin-fixed, paraffin-embedded tissues of the aforementioned mice injected with Control sh and ObR sh MCF-7 cells. Of particular interest was the finding of a significant reduction in SCD expression in formalin-fixed, paraffin-embedded tissues from mice injected with ObR sh MCF-7 breast cancer cells with respect to the control counterpart, as revealed by immunohistochemical staining (Figure 2I). These latter results further support the existence of a cooperative axis between SCD and LEP signaling, also in animal models.

SCD is abundantly expressed in hepatic and adipose tissues and is primarily controlled at the transcriptional level by SREBP-1 through interaction with a sterol response element within the promoter region of the *SDC* gene.[64–66] Previous studies have demonstrated that several hormonal factors, including 17β-estradiol and leptin, impact SCD transcription via SREBP-1 in various experimental models.[31,36] Thus, to explore the potential mechanism contributing to leptin's modulation of SCD in ERα-positive breast cancer cells, the expression levels of SREBP-1, the master transcription factor orchestrating lipid metabolism and SCD regulation, have been first assessed. It has been found that leptin exposure led to a marked increase

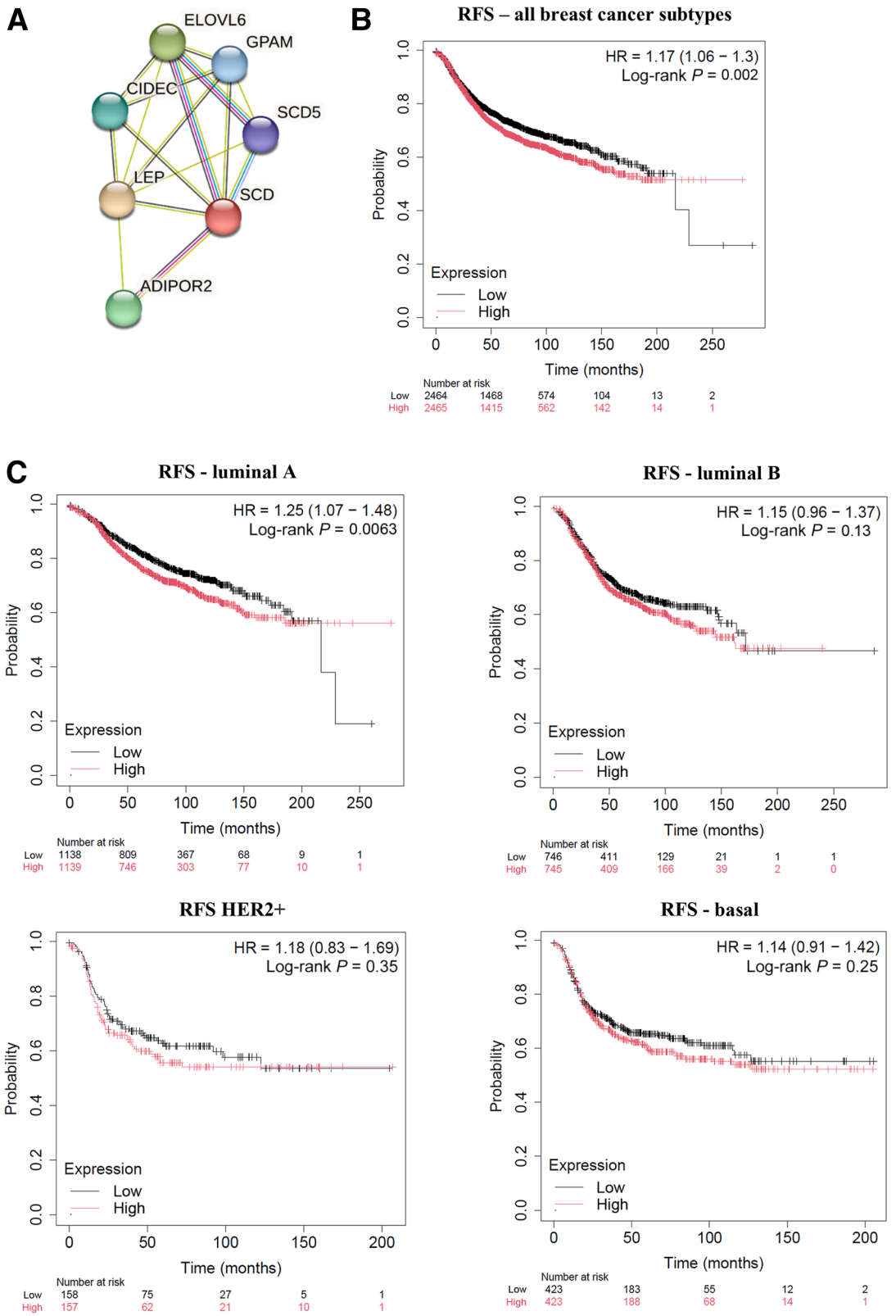

Figure 1 *In silico* analysis reveals a potential interplay between LEP and SCD. **A:** Protein-protein interaction (PPI) network of LEP and SCD. Only proteins with an interaction are shown and gave total seven nodes; there are 16 edges with an average node degree of 4.57 and PPI enrichment *P* value of 0.000124. **B** and **C:** Kaplan-Meier survival analysis of recurrence-free survival (RFS) rate in all breast cancer subtypes (**B**), or in patients with breast cancer classified according to the St. Gallen criteria into the following subtypes: luminal A, luminal B, human epidermal growth factor receptor 2 $(HER2)^{+}$, and basal subtypes (**C**), based on the mean co-expression levels of *LEP* and *SCD*. HR, hazard ratio; LEP, leptin; SCD, stearoyl-CoA desaturase.

in SREBP-1 expression, accompanied by a concomitant increase in the levels of the SREBP1 downstream target SCD (Figure 2J). *SREBP1* genetic silencing by siRNA impaired the leptin-driven SCD up-regulation (Figure 2J), indicating how leptin induction of SCD may occur via SREBP activation.

Effects of Leptin/SCD Axis on Cell Lipid Mass and Composition

Reminiscent of previous microarray analysis on the role of LEP in modulating the genome of MCF-7 cells (EBI ArrayExpress database, accession number: E-MTAB-3641, *https://www.ebi.ac.uk/biostudies/ArrayExpress/studies/E-MTAB-3641?query=E-MTAB-3641*,[38] last accessed December 15, 2024), an up-regulation of *SCD* was revealed in MCF-7 cells treated with LEP (fold change = 2.14, $P = 0.002$). To ensure robust statistical analysis for a next interactomics investigation, the data set of the detected and quantified expressed genes has been reprocessed by using linear Bayesian statistics. Differential expression between LEP-treated cells and control MCF-7 cells was evaluated according to the thresholds $-1 \geq \log2$ fold change ≥ 1 and false discovery rate ≤ 0.002, and 1003 DEGs were retrieved. Then, to investigate the potential role of SCD in the core interactome of DEG-coded proteins, a DIN 2 was generated by applying the MetaCore network building tool. Of the 965 DEG-coding proteins, reported in Supplemental Table S1 (EBI ArrayExpress database, accession number: E-MTAB-3641),[38] 813 DEGs-proteins (representing >80% of the total DEGs) were integrated into the DIN, hence stressing the reliability and relevance of the acquired data. Steroid hormone receptor estrogen-related receptor 1 (ERR1) (*ESRRA* in the DIN), transcription factor JunB (*JunB*), POU (Pit-Oct-Unc) domain, class 2, transcription factor 1 (*POU2F1*; *Oct-1* in the DIN), polycomb protein SUZ12 (*SUZ12*), and transcription factor p65 [also known as NF-κB p65 subunit (*RELA*); *RelA* (p65 NF-κB subunit) in the DIN] resulted the main central hubs of the net, as shown in Supplemental Figure S2A. Remarkably, SCD directly interacts with JunB and POU2F1 and indirectly i) with ERR1, through its interactors p300, oxysterols receptor liver X receptor (LXR)-β (LXR-β in the DIN) and CDK9; ii) with RELA, through p300, tryptophan-aspartic acid (WD) repeat-containing protein 5 (WDR5), CDK9, and heterogeneous nuclear ribonucleoprotein A1; and iii) with SUZ12, through p300 and WDR5. As a result, SCD was located in the innermost shell of the main central hub interactors, according to the organic hub-centric network layout (Supplemental Figure S2A). This suggests that the enzyme may exert a critical function, in coordination with the main central hubs, in the response of tumor cells to LEP stimulation. Blue bold vectors of Supplemental Figure S2A show the tight crosstalk among main central hubs, SCD, and SCD direct interactors (ie, p300, WDR5, LXR-β, CDK9, and heterogeneous nuclear ribonucleoprotein A1). Interestingly, the vast majority of these factors are known to play a role in the regulation of energy metabolism, principally lipid, glucose, and mitochondrial metabolism (ERR1; LXR-β; CDK9; RELA; and p300), as well as in its reprogramming in cancer cells (ERR1; POU2F1; CDK9; heterogeneous nuclear ribonucleoprotein A1; and p300).[67–82] Interactomics analysis hence highlighted the LEP/SCD axis centered in metabolism regulation, a finding further stressed by the enrichment analysis performed on DEG-coded proteins (Supplemental Figure S2B).

Consistent with these findings, the enrichment analysis associated to the SCD known interactors, which were retrieved from the dedicated STRING database and used for the SCD-PPI network generation via the single protein by name search, reported in Supplemental Figure S3A, recognized fatty acid biosynthetic process ranking among the most relevant biological process (Supplemental Figure S3B). In addition, acyl-CoA desaturase activity emerged as one of the most relevant molecular functions (Supplemental Figure S3C), whereas fatty acid elongase complex resulted in the main cellular-component enriched term (Supplemental Figure S3D). Accordingly, the biosynthesis of unsaturated fatty acids stood out as the most enriched Kyoto Encyclopedia of Genes and Genomes pathway (Supplemental Figure S3E).

In reason of the predicted metabolism modulation exerted by LEP through SCD, a detailed lipidomic analysis was conducted, primarily focusing on the fatty acid qualitative composition of diverse cell lipid classes, in MCF-7 breast cancer cells treated with LEP, with or without the SCD inhibitor MF-438.[19,83] Because SCD catalyzes the desaturation of SFAs, specifically palmitic acid (C16:0) and stearic acid (C18:0), into their respective monounsaturated counterparts (MUFA), palmitoleic acid (C16:1) and oleic acid (C18:1), the relative percentage of each fatty acid was quantified, as well as the proportion of fatty acids categorized according to their degree of unsaturation (SFA, MUFA, and polyunsaturated fatty acids), after 3 or 6 days of treatment with vehicle (−) or LEP (500 ng/mL) and with or without MF-438 (5 μmol/L). Treatment with LEP alone or in combination with MF-438 does not alter free cholesterol, CE, and TG masses in MCF-7 cells (Figure 3, A–C). The profile of the fatty acids contained in total lipid extracts was also analyzed, which also comprise lipid subclasses, such as phospholipids, diglycerides, and monoglycerides, beyond CE, free FA, and TG. Fatty acids from total lipid extracts range from C15:0 to C20:4, with obvious prevalence of C16:0, C18:0, and C18:1. When analyzing single fatty acids, after 3 days of treatment, no significant differences were appreciated, except for a switch in the relative abundance of C16:0 and C18:0, which decrease and increase, respectively, only after MF-438 treatment (Figure 3D). Because these fatty acids are both saturated, no differences were seen when fatty acids were categorized on the basis of their degree of unsaturation (Figure 3E). On the other hand, the profile was altered after 6 days of incubation with LEP (alone or with MF-438). In

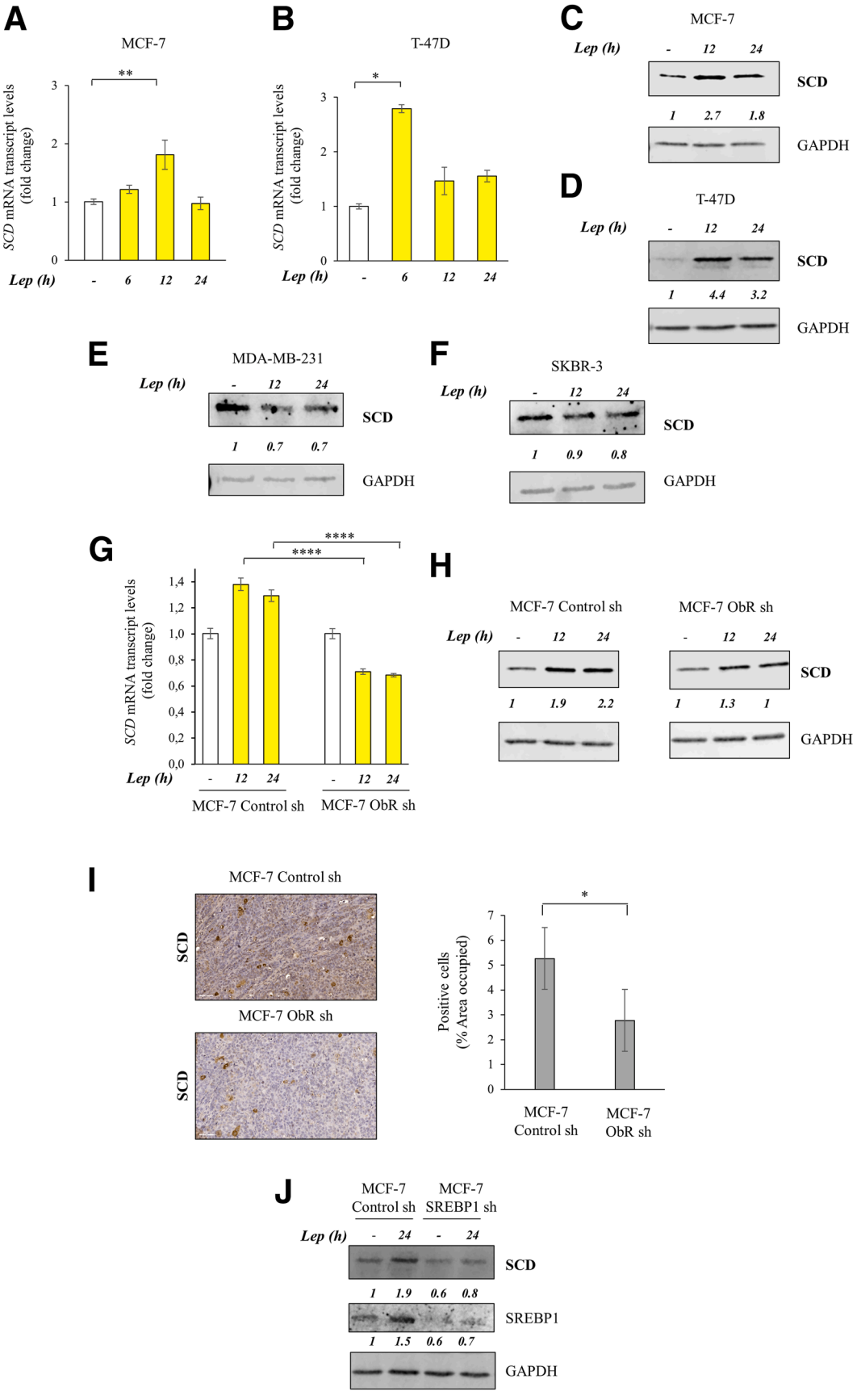
A
MCF-7
SCD mRNA transcript levels (fold change)
Lep (h)
B
T-47D
C
MCF-7
SCD
GAPDH
D
T-47D
E
MDA-MB-231
F
SKBR-3
G
MCF-7 Control sh
MCF-7 ObR sh
H
I
Positive cells (% Area occupied)
J
MCF-7 Control sh
MCF-7 SREBP1 sh
SREBP1

detail, LEP significantly decreased C16:0 and C18:0, with a concomitant increase in C18:1 (Figure 3F). Obviously, the effect was mirrored by a decrease in SFA and an increase in MUFA (Figure 3G), whereas no differences have been detected in polyunsaturated fatty acid profile. MF-438 prevented LEP-mediated effects in MUFAs. To further evaluate which lipid class may be mainly involved in this switch toward a higher degree of unsaturation, the fatty acid profile of CE and TG was analyzed. After 3 days of incubation, LEP decreased CE 16:0 and C18:0, whereas it concomitantly increased C18:1 (Figure 3H). This effect was significantly prevented by the addition of MF-438. The overall picture representing the switch toward a more MUFA profile and the MF-438–induced prevention is well depicted in Figure 3I. Interestingly, LEP seemed to lose its activity on CE profile after 6 days of treatment, where the tendency in SFA decrease and MUFA increase was still present (mainly because of C18:0 lowering) but not significant (Figure 3, J and K). Finally, LEP increased TG MUFAs, while it increased MUFA after 3 days of incubation. This effect was strongly prevented, or even counterbalanced, by MF-438, which significantly enhanced C18:0, with a concomitant decrease of C18:1 (Figure 3, L and M). As previously demonstrated for CE, also in TG, these effects were no longer noticeable after 6 days of treatment (Figure 3, N and O). In conclusion, lipidomic analysis showed that leptin promotes a shift toward MUFA production, an effect reversed by the SCD inhibitor MF-438, thereby confirming SCD dependency. From a functional point of view, SCD-1 activity may support tumor cell growth by increasing MUFA levels, which have been highlighted as a common hallmark of cancer cells.[84]

SCD Drives Leptin-Induced Mitochondrial Bioenergetics in ERα-Positive Breast Cancer Cells

In the light of the aforementioned data, it was further substantiated that SCD is a pivotal enzyme implicated in the transformation of SFAs, originating from *de novo* lipogenesis or dietary sources, into MUFAs. This further supports the previously reported significance of SCD as a crucial factor in maintaining metabolic homeostasis, with particular emphasis on its role in regulating lipid metabolism.[19,66,85] Moreover, it has been well documented that LEP is involved in metabolic reprogramming through consistent use of lipids for energy production. Specifically, there is mounting evidence that LEP primarily sustains mitochondrial metabolism in ER^+ breast cancer cells.[86–89] Consequently, the potential interplay between LEP and SCD also in modulating oxidative phosphorylation, the primary metabolic pathway through which cells produce energy, was investigated. To this end, it was evaluated whether inhibition of SCD expression and/or activity by pharmacologic or genetic approaches may reverse LEP-mediated effects. First, the specific inhibitor MF-438 was used, and the effects of LEP on several parameters associated with mitochondrial functions (basal and maximal respiration) were assessed. The OCR was measured directly in a Seahorse XFe 96 metabolic analyzer via the sequential injection of various cellular respiration modulators (oligomycin, rotenone/antimycin A, and FCCP). As expected, LEP treatment resulted in a substantial increase in mitochondrial respiration in MCF-7 cells, as evidenced by the elevated OCR in both basal and maximal conditions. Interestingly, the addition of the SCD inhibitor MF-438 effectively counteracted these changes, reducing OCR and basal and maximal respiration rates to levels comparable to the control group (Figure 4, A–C). These findings support the hypothesis that SCD activity is crucial for mediating the prometabolic effects of LEP. In accordance with these findings, it was observed that LEP treatment significantly increased ATP production, whereas these effects were completely abrogated by MF-438 (Figure 4D). Moreover, stable silenced SCD MCF-7 cells were generated using lentiviral transfection (Figure 5A). SCD silencing abrogated LEP effects on OCR and basal and maximal respiration rates (Figure 5, B–D). Consistently, LEP-mediated induction on ATP production was entirely abolished on SCD knockdown (Figure 5E), reinforcing the notion that SCD not only contributes to mitochondrial respiration but it is also required to sustain LEP-induced bioenergetics in breast cancer cells.

It is well established that increased ATP production is a key feature of proliferating and migrating cancer cells,

Figure 2 Leptin signaling pathway activation increases SCD expression in estrogen receptor (ER) α–positive MCF-7 and T-47D breast cancer cells. **A** and **B:** Quantitative real-time RT-PCR assay for *SCD* gene expression in ERα-positive MCF-7 (**A**) and T-47D (**B**) breast cancer cells treated with vehicle (–) or LEP (500 ng/mL) for 6, 12, and 24 hours. **C–F:** Immunoblotting showing SCD protein expression in MCF-7 (**C**), T-47D (**D**), MDA-MB-231 (**E**), and SKBR-3 (**F**) breast cancer cells treated with vehicle (–) or LEP (500 ng/mL) for 12 and 24 hours. Glyceraldehyde-3-phosphate dehydrogenase (GAPDH) was used as a control for equal loading and transfer. Italicized numbers below the blot represent the mean of the band OD expressed as fold over for vehicle-treated-cells. **G** and **H:** Quantitative real-time RT-PCR assay (**G**) and immunoblotting (**H**) for SCD mRNA and protein expression in ERα-positive MCF-7 empty vector control (Control sh) and stably silenced for ObR receptor (ObR sh) and treated with vehicle (–) or LEP (500 ng/mL) for 12 and 24 hours. GAPDH was used as a control for equal loading and transfer. Italicized numbers below the blot represent the mean of the band OD expressed as fold. The two images belong to the same blot. **I: Left panels:** Immunohistochemical (IHC) staining of SCD in MCF-7 Control sh and ObR sh xenograft tumor sections. **Right panel:** IHC relative score obtained by the ImageJ software version 1.52a, calculating the percentage of area occupied by SCD in six different sections of the same slide. The results were obtained from the mean of these values. **J:** Immunoblotting for SCD and sterol regulatory element–binding-protein-1 (SREBP1) expression in ERα-positive MCF-7 empty vector control (Control Sh) breast cancer cells and silenced for SREBP1 (SREBP1 sh) and treated with vehicle (–) or LEP (500 ng/mL) for 24 hours. GAPDH was used as a control for equal loading and transfer. Italicized numbers below the blot represent the mean of the band OD expressed as fold. The images belong to the same blot. $^*P < 0.05$, $^{**}P < 0.01$, and $^{****}P < 0.0001$. Scale bar = 70 μm (**I, left panels**).

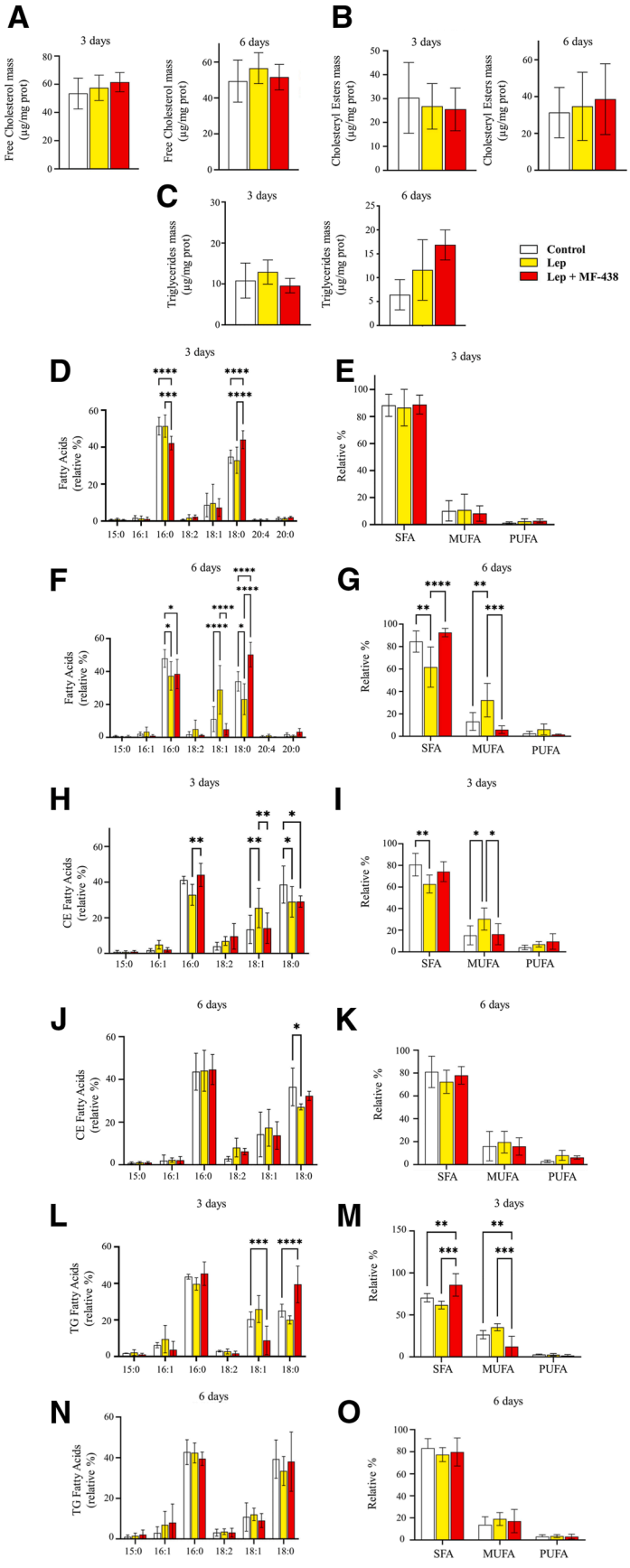
A
3 days
Free Cholesterol mass (µg/mg prot)
6 days
Free Cholesterol mass (µg/mg prot)
B
3 days
Cholesteryl Esters mass (µg/mg prot)
6 days
Cholesteryl Esters mass (µg/mg prot)
C
3 days
Triglycerides mass (µg/mg prot)
6 days
Triglycerides mass (µg/mg prot)
Control
Lep
Lep + MF-438
D
3 days
Fatty Acids (relative %)
15:0 16:1 16:0 18:2 18:1 18:0 20:4 20:0
E
3 days
Relative %
SFA MUFA PUFA
F
6 days
Fatty Acids (relative %)
15:0 16:1 16:0 18:2 18:1 18:0 20:4 20:0
G
6 days
Relative %
SFA MUFA PUFA
H
3 days
CE Fatty Acids (relative %)
15:0 16:1 16:0 18:2 18:1 18:0
I
3 days
Relative %
SFA MUFA PUFA
J
6 days
CE Fatty Acids (relative %)
15:0 16:1 16:0 18:2 18:1 18:0
K
6 days
Relative %
SFA MUFA PUFA
L
3 days
TG Fatty Acids (relative %)
15:0 16:1 16:0 18:2 18:1 18:0
M
3 days
Relative %
SFA MUFA PUFA
N
6 days
TG Fatty Acids (relative %)
15:0 16:1 16:0 18:2 18:1 18:0
O
6 days
Relative %
SFA MUFA PUFA

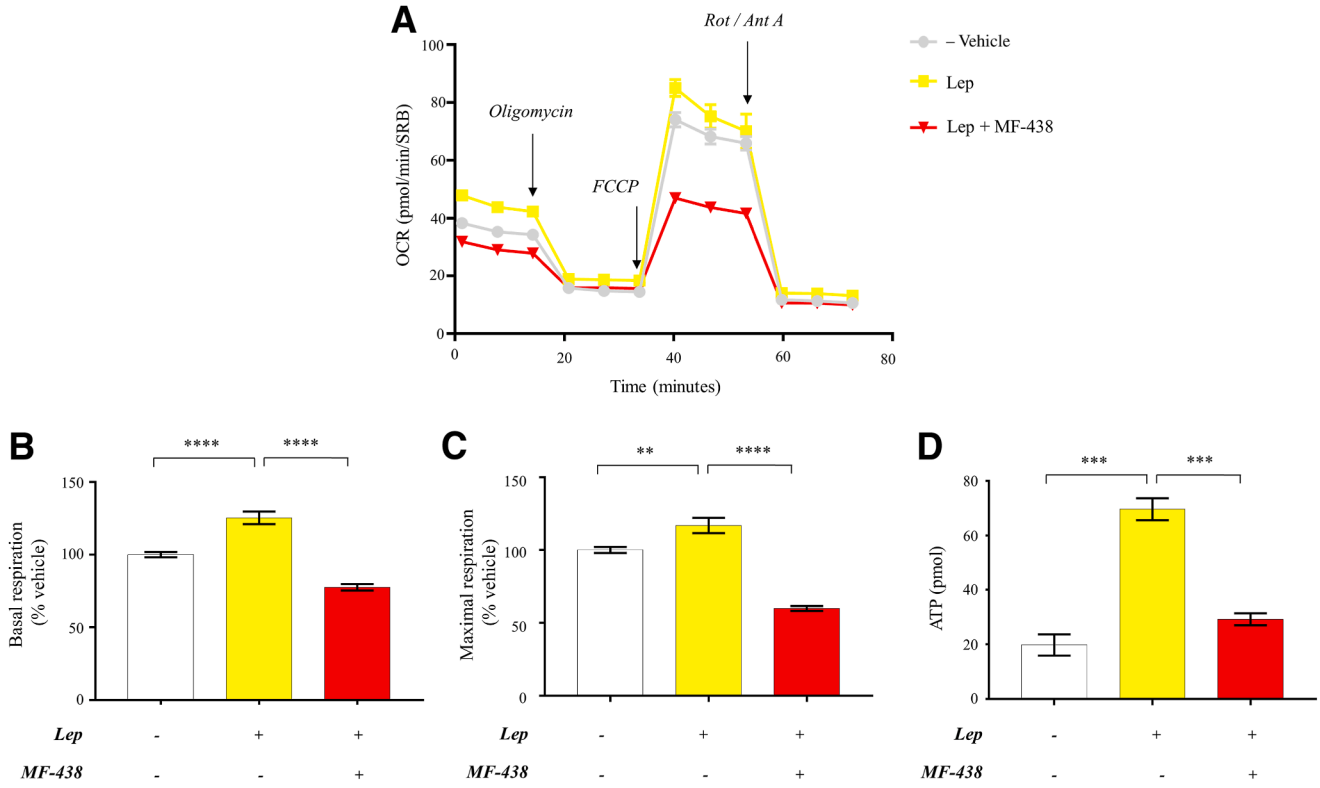

Figure 4 Pharmacologic SCD inhibition counteracts leptin-induced effects on mitochondrial metabolism and energy production in MCF-7 estrogen receptor α—positive breast cancer cells. **A—C:** Seahorse XF-e96 analyzer was used to measure the mitochondrial metabolic activity of MCF-7 cells treated with vehicle (—) or with LEP (500 ng/mL) in the presence or not of MF-438 (5 μmol/L) for 48 hours. Oxygen consumption rate (OCR) flux (**A**) and histograms of different mitochondrial respiratory parameters, such as basal (**B**) and maximal (**C**) respiration, are shown. Data were represented from five biological replicates from two independent experiments and normalized to protein content (sulforhodamine B assay). **D:** ATP production of MCF-7 cells treated with vehicle (—) or with LEP (500 ng/mL) in the presence or not of MF-438 (5 μmol/L) for 24 hours. Data were represented from three biological replicates from two independent experiments. Data are given as means ± SEM (**A—D**). $^{**}P < 0.01$, $^{***}P < 0.001$, and $^{****}P < 0.0001$.

providing the necessary energy to support biosynthetic processes, cytoskeletal remodeling, and motility.[90,91] On the other hand, targeting ATP synthase (ATPase) activity in cancer cells has been found to sensitize tumors to chemotherapeutic agents, enhancing the overall efficacy of treatment.[92,93] The therapeutic efficacy of ATPase inhibitors is attributed to their ability to disrupt lysosomal acidification, which is critical for cancer cell metabolism, survival, and drug resistance. In line with these observations, the ATPase inhibitors bedaquiline and oligomycin were able to reverse LEP-induced effects on growth (Supplemental Figure S4A) and migration (Supplemental Figure S4B) of ERα-positive MCF-7 breast cancer cells.

Collectively, these results emphasize the functional interaction between LEP and SCD in the metabolic regulation of ERα-positive breast cancer cells, providing further evidence of the critical role played by SCD in mediating the oncogenic effects of LEP.

SCD Inhibition Reverses Leptin-Induced Effects on Growth and Motility of ERα-Positive Breast Cancer Cells

Because changes in the metabolism of cancer cells represent a hallmark feature that is correlated with tumor initiation, progression, and metastases,[94] it was explored how the pharmacologic inhibition of SCD may counteract the well-known LEP-induced effects on breast cancer cell proliferation and migration. To this end, soft agar and wound healing assays were performed in ERα-positive MCF-7 and T47-D breast cancer cell lines, treated with LEP with or without the SCD inhibitor MF-438. As expected, a significant

Figure 3 Leptin amplifies the effects of SCD on the conversion of saturated fatty acids (SFAs) into monounsaturated fatty acids (MUFAs). **A—C:** Quantification of the mass of free (**A**) and esterified (**B**) cholesterol and triglycerides (**C**) of MCF-7 cells treated for 3 and 6 days with vehicle (—), or with LEP (500 ng/mL) in the presence or not of MF-438 (5 μmol/L). **D—G:** Fatty acid profile of total lipid extract from MCF-7 cells treated for 3 and 6 days with vehicle (—), or with LEP (500 ng/mL) in the presence or not of MF-438 (5 μmol/L). **H—K:** Fatty acid profile of cholesteryl ester (CE) extract of MCF-7 cells treated for 3 and 6 days with vehicle (—), or with LEP (500 ng/mL) in the presence or not of MF-438 (5 μmol/L). **L—O:** Fatty acid profile of triglyceride (TG) extract from MCF-7 cells treated for 3 and 6 days with vehicle (—), or with LEP (500 ng/mL) in the presence or not of MF-438 (5 μmol/L). $^{*}P < 0.05$, $^{**}P < 0.01$, $^{***}P < 0.001$, and $^{****}P < 0.0001$.

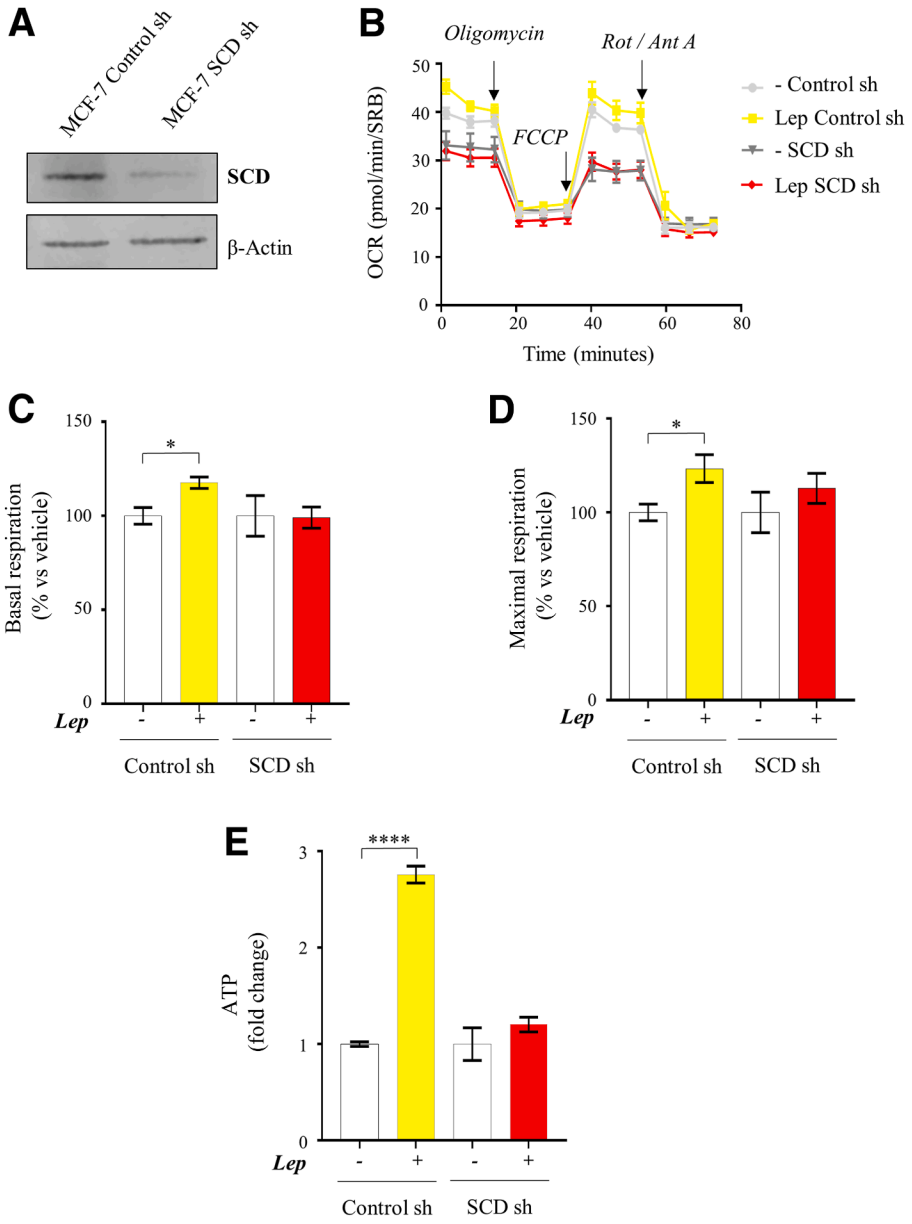

Figure 5 SCD silencing counteracts leptin-induced effects on mitochondrial metabolism and energy production in MCF-7 estrogen receptor α—positive breast cancer cells. **A:** Immunoblotting showing SCD protein expression in Control sh and SCD sh MCF-7 cells. Glyceraldehyde-3-phosphate dehydrogenase was used as a control for equal loading and transfer. Seahorse XF-e96 analyzer was used to measure the mitochondrial metabolic activity of Control sh and SCD sh MCF-7 cells treated with vehicle (—) or with LEP (500 ng/mL) for 48 hours. **B—D:** Oxygen consumption rate (OCR) flux (**B**) and histograms of different mitochondrial respiratory parameters, such as basal (**C**) and maximal (**D**) respiration, are shown. Data were represented from five biological replicates from two independent experiments and normalized to protein content (sulforhodamine B assay). **E:** ATP production of Control sh and SCD sh MCF-7 cells treated with vehicle (—) or with LEP (500 ng/mL). Data were represented from three biological replicates from two independent experiments. Data are given as means ± SEM (**B—E**). $*P < 0.05$, $****P < 0.0001$.

increase in colony numbers was found in both MCF-7 and T47-D cells treated with LEP, whereas treatment with MF-438 completely abrogated these effects (Figure 6, A and B). Wound healing assay confirmed anchorage-independent soft agar growth results, indicating a significant LEP-mediated induction of cell motility, which is effectively counteracted by MF-438 treatment (Figure 6, C and D).

Finally, it was found that LEP treatment was not able to increase cell growth and motility of MCF-7 breast cancer cells in the presence of SCD silencing (Figure 6, E and F), further corroborating the role of SDC in mediating LEP protumorigenic functions.

Discussion

Breast cancer is the most frequently diagnosed malignancy worldwide and continues to be a major cause of cancer-

related mortality.[1] This neoplasm is characterized by significant heterogeneity and is primarily categorized into four distinct classifications based on the expression of specific receptors: luminal A, luminal B, HER2 enriched, and triple-negative or basal-like subtypes. Luminal A tumors, defined by high ER and progesterone receptor expression without HER2 amplification, are the most common molecular subtype of breast cancer, accounting for 60% to 70% of all cases.[95,96] Furthermore, this subtype demonstrates a marked dependence on hormonal and metabolic pathways for their growth and progression. Importantly, obesity, one the most common metabolic diseases and a major global health concern, has been consistently demonstrated to be a significant risk factor for ERα^+ breast cancers. The molecular mechanisms underpinning this association are currently an important focus of investigation. In the present study, it was demonstrated that the interaction between the obesity-derived adipokine leptin and SCD, a critical enzyme in lipid metabolism often associated with the development of obesity, supports the growth and migration of luminal A-like breast cancer cells.

Studies have identified an increased expression of SCD in human patient tumors, including those of the breast, prostate, lung, ovary, endometrium, bladder, thyroid, colon, and kidney, in comparison with the corresponding normal tissues.[97–102] Specifically, SCD was found to be overexpressed in immunohistochemical sections of breast cancer tissues in comparison with normal tissues. This finding was found to correlate with the elevated levels of MUFAs that were detected by mass spectrometry analysis in the cancerous area in comparison with the adjacent normal area in breast cancer tissue.[97] Interestingly, a reverse phase protein array revealed elevated levels of SCD in ER$^+$ breast tumors in comparison to triple-negative breast cancers. Furthermore, these increased levels of SCD were found to be associated with significantly reduced relapse-free survival and overall survival, as determined by multivariable analysis.[23] *In vitro* evidence reported that SCD is involved in modulating growth and progression of breast cancer cells. In fact, it has been demonstrated that the small-molecule SCD inhibitor, CVT-11127, reduced the proliferation of breast cancer cells.[103] Moreover, it has been documented that the genomic inhibition of SCD resulted in the impairment of the Wnt/β-catenin signaling pathway, thereby interfering with the epithelial-to-mesenchymal transition in breast cancer cells.[104] SCD also confers resistance to breast cancer cells towards reactive oxygen species–induced ferroptosis and modulates the stress response pathways that contribute to their growth and metastatization.[105] It is noteworthy that SCD has been identified as a possible key signaling axis within the tumor microenvironment. In particular, it has been hypothesized that a potential interplay exists between cancer-associated fibroblast–derived soluble factors, such as hepatocyte growth factor, transforming growth factor-β, and basic fibroblast growth factors and SCD in mediating the migratory capabilities of MCF-7 breast cancer cells sustained by cancer-associated fibroblasts.[106] Consistent with these findings, additional data have shown that SCD expression is modulated by transforming growth factor-β and other growth factors, such as platelet-derived growth factor, along with hormones, including thyroid hormone, insulin, and estrogen.[31,107–111] Here, it was demonstrated that SCD was also a target of the obesity-derived hormone leptin in ERα-positive breast cancer cells. It was found that LEP induced a time-dependent up-regulation of SCD expression at both the transcript and protein levels in two different ERα^+ luminal-like breast cancer cells (namely, MCF-7 and T-47D cells). It is noteworthy that the integrity of LEP/ObR signaling is necessary for SCD up-regulation. Immunoblot and quantitative real-time RT-PCR analyses revealed that LEP was no longer able to increase SCD expression in MCF-7 cells in which the ObR was silenced at the genomic level. Furthermore, immunohistochemical analysis of xenograft tumor sections from mice implanted with the same ObR sh stable clones clearly showed a reduction in SCD expression compared with the control counterpart. The aforementioned process may be initiated by the up-regulation of SREBP-1, a pivotal transcriptional factor that has been demonstrated to regulate SCD expression, as a consequence of leptin stimulation. The effect of LEP on SCD expression depends on the specific cellular background, as SCD expression has not been demonstrated to be up-regulated in the triple-negative basal-like MDA-MB-231 and ER-negative/HER2-overexpressing SKBR-3 breast cancer cell lines. More interesting, these findings indicate that SCD was important in mediating the protumoral effects of LEP. Indeed, the genetic or pharmacologic inhibition of SCD using a lentiviral approach or the specific MF-438 drug, respectively, has been shown to abrogate the LEP-induced effects on proliferation and migration of both ERα-positive MCF-7 and T-47D breast cancer cells. Finally, it was also shown that elevated expression levels of LEP and SCD correlate with poorer recurrence-free survival exclusively in patients with luminal A breast cancer, thus indicating that the interplay between LEP and SCD could be subtype specific.

The primary function of SCD is to modulate the conversion of SFAs into MUFAs; thus, the presence of decreased levels of SFAs and increased levels of MUFAs is indicative of SCD enzymatic activity.[16] Interestingly, lipidomic analysis revealed that LEP treatment induces a qualitative shift in FA profiles, by decreasing levels of SFAs and increasing MUFAs. These effects were abrogated by the use of MF-438, thereby confirming the dependency of LEP-induced lipid reprogramming on SCD. Furthermore, the levels of triglycerides and cholesterol esters remained largely unaltered, indicating that LEP exerts its influence predominantly on the composition of

lipids rather than on their total abundance. It is worthwhile to underline that SCD inhibition plays a different time-dependent effect based on the analyzed lipid subclass. Quicker effects are already evident (3 days) in TG and CE, whereas those on total lipids (ie, phospholipids) are significant only after a 6 days of treatment. This is consistent with the half-life and with the relative turnover of these subclasses.

Lipid metabolism (synthesis and enhanced uptake) is a fundamental process within the context of cancer biology

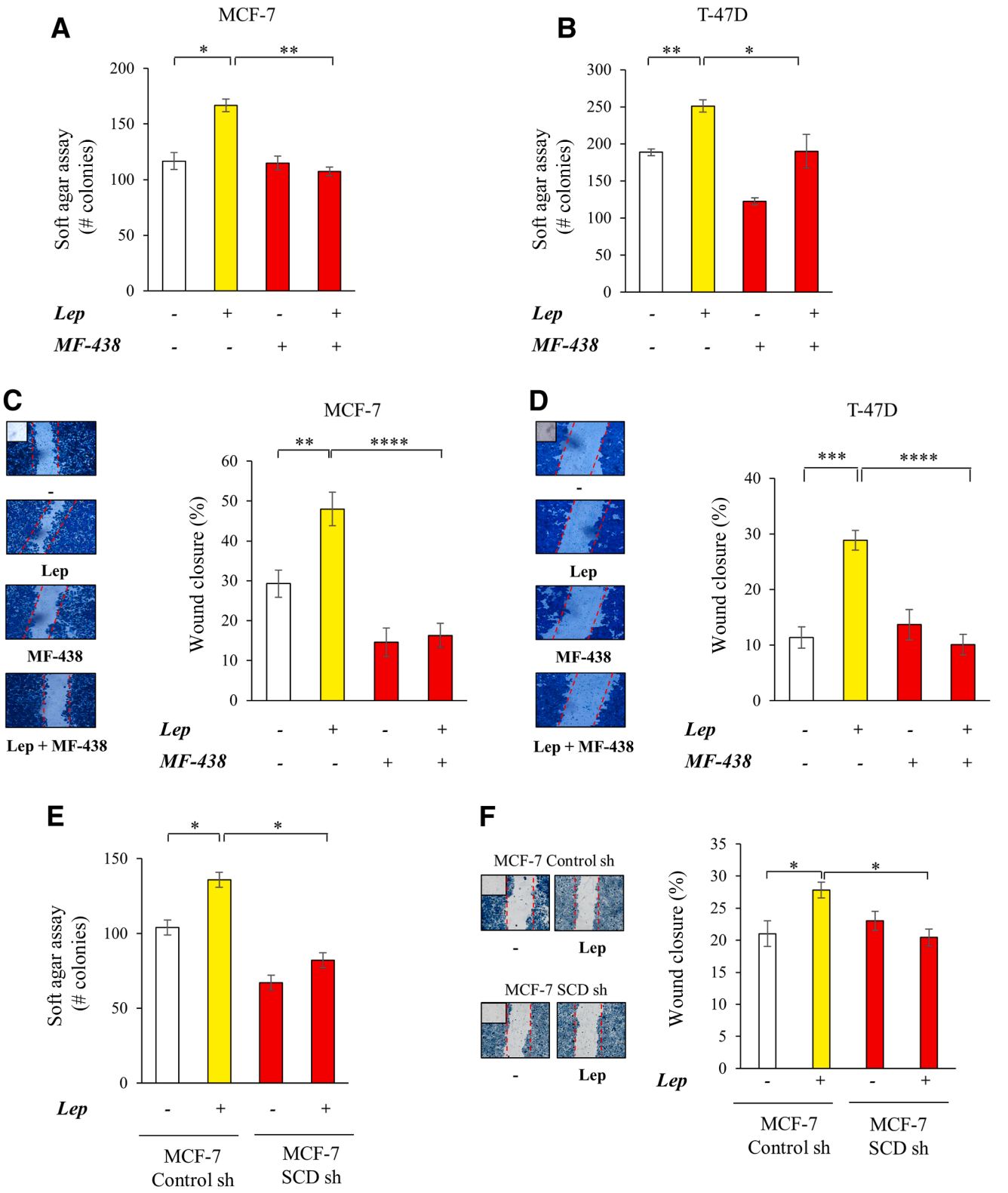

supporting membrane biosynthesis, energy storage and production, and generation of signaling intermediates.[112,113] Evidence suggests a correlation between the presence of saturated and unsaturated lipids and cancer progression. Indeed, it has been demonstrated that SFAs can trigger an endoplasmic reticulum stress response, which may inhibit tumor growth. Conversely, a correlation has been established between MUFAs and the development of cancer, unfavorable prognoses, and increased mortality rates.[84,114,115] In a molecular point of view, SFAs impact cellular function via effects on membrane properties, and also influencing intracellular signaling and gene transcription (ie, Wnt signaling pathway, Akt/glycogen synthase kinase 3β/β-catenin signaling), because they exhibit a higher rate of esterification with respect to SFAs of similar chain length because of their major binding affinity to the cytosolic FA-binding proteins.[116] Furthermore, it has been widely documented that abnormalities in lipid metabolism are prevalent among obese patients.[117] In the context of obesity-related factors, LEP plays a pivotal role in the metabolic process, encompassing the processes of lipid metabolism.[87,118–120] It has been previously reported that LEP affects cell metabolism by inducing the secretion of extracellular vesicles enriched with proteins associated with metabolic processes. Specifically, it was observed that LEP-derived extracellular vesicles induced a metabolic shift in breast cancer cells and macrophages toward oxidative phosphorylation, thereby contributing to the aggressive behavior of epithelial cells and the protumoral phenotype of immune cells.[89] Here, it was found that the pharmacologic inhibition of SCD using MF-438 abrogated the LEP-induced effects on both basal and maximal respiration, as evidenced by Seahorse metabolic profile. These findings are consistent with the ability of MF-438 to restore ATP levels to baseline conditions, thereby counteracting the effects of LEP in sustaining energy production in MCF-7 breast cancer cells. In line with this evidence, it has been determined that the genetic inhibition of SCD also counteracted the leptin-induced effects on mitochondrial metabolism and energy production. Noteworthy, these processes depend on functional mitochondria and ATPase. In the past two decades, many oxidative phosphorylation complex inhibitors have been developed as potential treatments and involved in several clinical trials for cancer therapy.[121–124] If ATPase is inhibited (eg, with oligomycin or bedaquiline), leptin-induced metabolic benefits, like mitochondrial biogenesis and lipid catabolism, are suppressed, thereby reducing anchorage-independent growth and migration of MCF-7 breast cancer cells.

The results obtained highlight the pivotal role of SCD in orchestrating metabolic adaptations induced by LEP, which facilitate tumor growth. In addition, these findings suggest that the inhibition of the LEP/SCD axis may result in the identification of new potential therapeutic targets. Further validation in patient-derived models or prospective clinical studies will be essential to confirm the clinical relevance of these findings, potentially providing evidence for a causal role of this axis in human breast cancer progression.

Collectively, these findings suggest that the LEP/SCD axis could be a key driver of tumor progression and metabolic reprogramming in ERα-positive breast cancer, providing a further molecular connection between obesity-associated factors and breast cancer biology. By targeting SCD, it may be possible to disrupt this axis, thereby mitigating the protumorigenic effects of LEP and addressing the metabolic vulnerabilities of obesity-driven breast cancer. The elucidation of this novel mechanistic framework linking obesity to breast cancer progression identifies potential promising therapeutic targets (ie, SCD), with the ultimate goal of improving outcomes for patients experiencing obesity-driven ERα-positive breast cancer.

Author Contributions

F.M.A., L.G., S.C., and I.B. conceptualized the study, visualized the data, developed methods, wrote the manuscript, and supervised the study; S.C., I.B., L.Bi., L.A., A.Co., C.G., D.B., and S.A. reviewed and edited the manuscript; F.M.A., L.G., L.M., P.D.C., L.Ba., A.Ca., R.D.S., L.A., A.E.L., and R.M. performed investigations and formal analysis; L.G., I.B., L.Bi., C.G., D.B., M.F., and M.P.L. curated data and visualized and validated data; and all authors reviewed and approved the final manuscript.

Disclosure Statement

None declared.

Figure 6 SCD inhibition abrogates leptin-mediated effects on growth and migration of estrogen receptor (ER) α–positive breast cancer cells. **A** and **B:** Anchorage-independent soft agar growth assay in ERα-positive MCF-7 (**A**) and T-47D (**B**) breast cancer cells treated with vehicle (−), LEP (500 ng/mL), and/or MF-438 (5 μmol/L). Values are represented as a mean of colonies number >50 μm diameter counted at the end of assay. **C** and **D:** Wound healing assay in ERα-positive MCF-7 (**C**) and T-47D (**D**) breast cancer cells treated with vehicle (−), LEP (500 ng/mL), and/or MF-438 (5 μmol/L). **Left panels:** Representative images. The wound's perimeter was delineated by the presence of **red lines**. **Right panels:** Histograms representing the relative percentage of wound closure calculated by ImageJ version 1.52a. The values represent the data from two to three different experiments. **E:** Soft agar growth assay in Control sh and SCD sh MCF-7 cells treated with vehicle (−) or LEP (500 ng/mL). Values are represented as a mean of colonies number >50 μm diameter counted at the end of assay. **F:** Wound healing assay in Control EV and SCD sh MCF-7 cells treated with vehicle (−) or LEP (500 ng/mL). **Left panels:** Representative images. The wound's perimeter was delineated by the presence of **red lines**. **Right panel:** Histograms representing the relative percentage of wound closure calculated by ImageJ. The values represent the data from two to three different experiments. Data are given as means ± SEM (**A**–**F**). *$P < 0.05$, **$P < 0.01$, ***$P < 0.001$, and ****$P < 0.001$.

Supplemental Data

Supplemental material for this article can be found at *https://doi.org/10.1016/j.ajpath.2025.08.009*.

References

1. Katsura C, Ogunmwonyi I, Kankam HK, Saha S: Breast cancer: presentation, investigation and management. Br J Hosp Med (Lond) 2022, 83:1–7
2. Arneth B: Tumor microenvironment. Medicina (Kaunas) 2019, 56: 15
3. Barone I, Caruso A, Gelsomino L, Giordano C, Bonofiglio D, Catalano S, Andò S: Obesity and endocrine therapy resistance in breast cancer: mechanistic insights and perspectives. Obes Rev 2022, 23:e13358
4. Andò S, Gelsomino L, Panza S, Giordano C, Bonofiglio D, Barone I, Catalano S: Obesity, leptin and breast cancer: epidemiological evidence and proposed mechanisms. Cancers (Basel) 2019, 11:62
5. Iyengar NM, Gucalp A, Dannenberg AJ, Hudis CA: Obesity and cancer mechanisms: tumor microenvironment and inflammation. J Clin Oncol 2016, 34:4270–4276
6. Quail DF, Dannenberg AJ: The obese adipose tissue microenvironment in cancer development and progression. Nat Rev Endocrinol 2019, 15:139–154
7. Caruso A, Gelsomino L, Panza S, Accattatis FM, Naimo GD, Barone I, Giordano C, Catalano S, Andò S: Leptin: a heavyweight player in obesity-related cancers. Biomolecules 2023, 13:1084
8. Sánchez-Jiménez F, Pérez-Pérez A, de la Cruz-Merino L, Sánchez-Margalet V: Obesity and breast cancer: role of leptin. Front Oncol 2019, 9:596
9. Becerril S, Rodríguez A, Catalán V, Ramírez B, Unamuno X, Portincasa P, Gómez-Ambrosi J, Frühbeck G: Functional relationship between leptin and nitric oxide in metabolism. Nutrients 2019, 11:2129
10. Pereira S, Cline DL, Glavas MM, Covey SD, Kieffer TJ: Tissue-specific effects of leptin on glucose and lipid metabolism. Endocr Rev 2021, 42:1–28
11. Stern JH, Rutkowski JM, Scherer PE: Adiponectin, leptin, and fatty acids in the maintenance of metabolic homeostasis through adipose tissue crosstalk. Cell Metab 2016, 23:770–784
12. Hanahan D: Hallmarks of cancer: new dimensions. Cancer Discov 2022, 12:31–46
13. Wang Y-P, Lei Q-Y: Perspectives of reprogramming breast cancer metabolism. Adv Exp Med Biol 2017, 1026:217–232
14. Kubota CS, Espenshade PJ: Targeting stearoyl-CoA desaturase in solid tumors. Cancer Res 2022, 82:1682–1688
15. Paton CM, Ntambi JM: Biochemical and physiological function of stearoyl-CoA desaturase. Am J Physiol Endocrinol Metab 2009, 297: E28–E37
16. Tracz-Gaszewska Z, Dobrzyn P: Stearoyl-CoA desaturase 1 as a therapeutic target for the treatment of cancer. Cancers (Basel) 2019, 11:948
17. Huang J, Fan X-X, He J, Pan H, Li R-Z, Huang L, Jiang Z, Yao X-J, Liu L, Lai-Han Leung E, He J-X: SCD1 is associated with tumor promotion, late stage and poor survival in lung adenocarcinoma. Oncotarget 2016, 7:39970–39979
18. Ran H, Zhu Y, Deng R, Zhang Q, Liu X, Feng M, Zhong J, Lin S, Tong X, Su Q: Stearoyl-CoA desaturase-1 promotes colorectal cancer metastasis in response to glucose by suppressing PTEN. J Exp Clin Cancer Res 2018, 37:54
19. Sen U, Coleman C, Sen T: Stearoyl coenzyme A desaturase-1: multitasker in cancer, metabolism, and ferroptosis. Trends Cancer 2023, 9:480–489
20. Wang J, Xu Y, Zhu L, Zou Y, Kong W, Dong B, Huang J, Chen Y, Xue W, Huang Y, Zhang J: High expression of stearoyl-CoA desaturase 1 predicts poor prognosis in patients with clear-cell renal cell carcinoma. PLoS One 2016, 11:e0166231
21. Wang L, Ye G, Wang Y, Wang C: Stearoyl-CoA desaturase 1 regulates malignant progression of cervical cancer cells. Bioengineered 2022, 13:12941–12954
22. Ascenzi F, De Vitis C, Maugeri-Saccà M, Napoli C, Ciliberto G, Mancini R: SCD1, autophagy and cancer: implications for therapy. J Exp Clin Cancer Res 2021, 40:265
23. Holder AM, Gonzalez-Angulo AM, Chen H, Akcakanat A, Do K-A, Fraser Symmans W, Pusztai L, Hortobagyi GN, Mills GB, Meric-Bernstam F: High stearoyl-CoA desaturase 1 expression is associated with shorter survival in breast cancer patients. Breast Cancer Res Treat 2013, 137:319–327
24. Peck B, Schug ZT, Zhang Q, Dankworth B, Jones DT, Smethurst E, Patel R, Mason S, Jiang M, Saunders R, Howell M, Mitter R, Spencer-Dene B, Stamp G, McGarry L, James D, Shanks E, Aboagye EO, Critchlow SE, Leung HY, Harris AL, Wakelam MJO, Gottlieb E, Schulze A: Inhibition of fatty acid desaturation is detrimental to cancer cell survival in metabolically compromised environments. Cancer Metab 2016, 4:6
25. Sun Y-S, Zhao Z, Yang Z-N, Xu F, Lu H-J, Zhu Z-Y, Shi W, Jiang J, Yao P-P, Zhu H-P: Risk factors and preventions of breast cancer. Int J Biol Sci 2017, 13:1387–1397
26. Morad V, Abrahamsson A, Dabrosin C: Estradiol affects extracellular leptin:adiponectin ratio in human breast tissue in vivo. J Clin Endocrinol Metab 2014, 99:3460–3467
27. Catalano S, Mauro L, Marsico S, Giordano C, Rizza P, Rago V, Montanaro D, Maggiolini M, Panno ML, Andó S: Leptin induces, via ERK1/ERK2 signal, functional activation of estrogen receptor [alpha] in MCF-7 cells. J Biol Chem 2004, 279:19908–19915
28. Lautenbach A, Budde A, Wrann CD, Teichmann B, Vieten G, Karl T, Nave H: Obesity and the associated mediators leptin, estrogen and IGF-I enhance the cell proliferation and early tumorigenesis of breast cancer cells. Nutr Cancer 2009, 61:484–491
29. Binai NA, Damert A, Carra G, Steckelbroeck S, Löwer J, Löwer R, Wessler S: Expression of estrogen receptor alpha increases leptin-induced STAT3 activity in breast cancer cells. Int J Cancer 2010, 127:55–66
30. Valle A, Sastre-Serra J, Oliver J, Roca P: Chronic leptin treatment sensitizes MCF-7 breast cancer cells to estrogen. Cell Physiol Biochem 2011, 28:823–832
31. Belkaid A, Duguay SR, Ouellette RJ, Surette ME: 17[beta]-Estradiol induces stearoyl-CoA desaturase-1 expression in estrogen receptor-positive breast cancer cells. BMC Cancer 2015, 15:440
32. Biddinger SB, Miyazaki M, Boucher J, Ntambi JM, Kahn CR: Leptin suppresses stearoyl-CoA desaturase 1 by mechanisms independent of insulin and sterol regulatory element–binding protein-1c. Diabetes 2006, 55:2032–2041
33. Thon M, Hosoi T, Chea C, Ozawa K: Loss of stearoyl-CoA desaturase-1 activity induced leptin resistance in neuronal cells. Biol Pharm Bull 2017, 40:1161–1164
34. Saxena NK, Sharma D, Ding X, Lin S, Marra F, Merlin D, Anania FA: Concomitant activation of the JAK/STAT, PI3K/AKT, and ERK signaling is involved in leptin-mediated promotion of invasion and migration of hepatocellular carcinoma cells. Cancer Res 2007, 67:2497–2507
35. Mauvoisin D, Prévost M, Ducheix S, Arnaud M-P, Mounier C: Key role of the ERK1/2 MAPK pathway in the transcriptional regulation of the stearoyl-CoA desaturase (SCD1) gene expression in response to leptin. Mol Cell Endocrinol 2010, 319:116–128
36. Luo S-D, Tsai H-T, Chiu T-J, Li S-H, Hsu Y-L, Su L-J, Tsai M-H, Lee C-Y, Hsiao C-C, Chen C-H: Leptin silencing attenuates lipid accumulation through sterol regulatory element-binding protein 1 inhibition in nasopharyngeal carcinoma. Int J Mol Sci 2022, 23: 5700

37. Gelsomino L, Naimo GD, Malivindi R, Augimeri G, Panza S, Giordano C, Barone I, Bonofiglio D, Mauro L, Catalano S, Andò S: Knockdown of leptin receptor affects macrophage phenotype in the tumor microenvironment inhibiting breast cancer growth and progression. Cancers (Basel) 2020, 12:2078
38. Giordano C, Chemi F, Panza S, Barone I, Bonofiglio D, Lanzino M, Cordella A, Campana A, Hashim A, Rizza P, Leggio A, Győrffy B, Simões BM, Clarke RB, Weisz A, Catalano S, Andò S: Leptin as a mediator of tumor-stromal interactions promotes breast cancer stem cell activity. Oncotarget 2016, 7:1262−1275
39. Love MI, Huber W, Anders S: Moderated estimation of fold change and dispersion for RNA-seq data with DESeq2. Genome Biol 2014, 15:550
40. Ritchie ME, Phipson B, Wu D, Hu Y, Law CW, Shi W, Smyth GK: limma powers differential expression analyses for RNA-sequencing and microarray studies. Nucleic Acids Res 2015, 43:e47
41. Xie Z, Bailey A, Kuleshov MV, Clarke DJB, Evangelista JE, Jenkins SL, Lachmann A, Wojciechowicz ML, Kropiwnicki E, Jagodnik KM, Jeon M, Ma'ayan A: Gene set knowledge discovery with Enrichr. Curr Protoc 2021, 1:e90
42. Lazzarato L, Bianchi L, Andolfo A, Granata A, Lombardi M, Sinelli M, Rolando B, Carini M, Corsini A, Fruttero R, Arnaboldi L: Proteomics studies suggest that nitric oxide donor furoxans inhibit in vitro vascular smooth muscle cell proliferation by nitric oxide-independent mechanisms. Molecules 2023, 28:5724
43. Bianchi L, Damiani I, Castiglioni S, Carleo A, De Salvo R, Rossi C, Corsini A, Bellosta S: Smooth muscle cell phenotypic switch induced by traditional cigarette smoke condensate: a holistic overview. Int J Mol Sci 2023, 24:6431
44. Bini L, Schvartz D, Carnemolla C, Besio R, Garibaldi N, Sanchez J-C, Forlino A, Bianchi L: Intracellular and extracellular markers of lethality in osteogenesis imperfecta: a quantitative proteomic approach. Int J Mol Sci 2021, 22:429
45. Győrffy B: Survival analysis across the entire transcriptome identifies biomarkers with the highest prognostic power in breast cancer. Comput Struct Biotechnol J 2021, 19:4101−4109
46. Mihály Z, Kormos M, Lánczky A, Dank M, Budczies J, Szász MA, Győrffy B: A meta-analysis of gene expression-based biomarkers predicting outcome after tamoxifen treatment in breast cancer. Breast Cancer Res Treat 2013, 140:219−232
47. Catalano S, Malivindi R, Giordano C, Gu G, Panza S, Bonofiglio D, Lanzino M, Sisci D, Panno ML, Andò S: Farnesoid X receptor, through the binding with steroidogenic factor 1-responsive element, inhibits aromatase expression in tumor Leydig cells. J Biol Chem 2010, 285:5581−5593
48. Committee for the Update of the Guide for the Care and Use of Laboratory Animals; National Research Council: Guide for the Care and Use of Laboratory Animals. Eighth Edition. Washington, DC, National Academies Press, 2011
49. Arnaboldi L, Ossoli A, Giorgio E, Pisciotta L, Lucchi T, Grigore L, Pavanello C, Granata A, Pasta A, Arosio B, Azzolino D, Baragetti A, Castelnuovo S, Corsini A, Catapano AL, Calabresi L, Gomaraschi M: LIPA gene mutations affect the composition of lipoproteins: enrichment in ACAT-derived cholesteryl esters. Atherosclerosis 2020, 297:8−15
50. Giordano C, Cui Y, Barone I, Ando S, Mancini MA, Berno V, Fuqua SAW: Growth factor-induced resistance to tamoxifen is associated with a mutation of estrogen receptor [alpha] and its phosphorylation at serine 305. Breast Cancer Res Treat 2010, 119: 71−85
51. Dogan S, Leopold J, Hoffmann DT, Kubitschke H, Blauth E, Ficorella C, Zschau A, Schiller J, Käs JA: Identification of lipid droplet-associated genes in breast cancer patients. Lipidology 2024, 1:52−74
52. Gupta A, Balakrishnan B, Karki S, Slayton M, Jash S, Banerjee S, Grahn THM, Jambunathan S, Disney S, Hussein H, Kong D, Lowell BB, Natarajan P, Reddy UK, Gokce N, Sharma VM, Puri V: Human CIDEC transgene improves lipid metabolism and protects against high-fat diet−induced glucose intolerance in mice. J Biol Chem 2022, 298:102347
53. Li Y, Kang H, Chu Y, Jin Y, Zhang L, Yang R, Zhang Z, Zhao S, Zhou L: Cidec differentially regulates lipid deposition and secretion through two tissue-specific isoforms. Gene 2018, 641:265−271
54. Feng Y-H, Chen W-Y, Kuo Y-H, Tung C-L, Tsao C-J, Shiau A-L, Wu C-L: Elovl6 is a poor prognostic predictor in breast cancer. Oncol Lett 2016, 12:207−212
55. Matsuzaka T, Shimano H, Yahagi N, Kato T, Atsumi A, Yamamoto T, Inoue N, Ishikawa M, Okada S, Ishigaki N, Iwasaki H, Iwasaki Y, Karasawa T, Kumadaki S, Matsui T, Sekiya M, Ohashi K, Hasty AH, Nakagawa Y, Takahashi A, Suzuki H, Yatoh S, Sone H, Toyoshima H, Osuga J, Yamada N: Crucial role of a long-chain fatty acid elongase, Elovl6, in obesity-induced insulin resistance. Nat Med 2007, 13:1193−1202
56. Muir K, Hazim A, He Y, Peyressatre M, Kim D-Y, Song X, Beretta L: Proteomic and lipidomic signatures of lipid metabolism in NASH-associated hepatocellular carcinoma. Cancer Res 2013, 73: 4722−4731
57. Brockmöller SF, Bucher E, Müller BM, Budczies J, Hilvo M, Griffin JL, Orešič M, Kallioniemi O, Iljin K, Loibl S, Darb-Esfahani S, Sinn BV, Klauschen F, Prinzler J, Bangemann N, Ismaeel F, Fiehn O, Dietel M, Denkert C: Integration of metabolomics and expression of glycerol-3-phosphate acyltransferase (GPAM) in breast cancer—link to patient survival, hormone receptor status, and metabolic profiling. J Proteome Res 2012, 11:850−860
58. Wendel AA, Lewin TM, Coleman RA: Glycerol-3-phosphate acyltransferases: rate limiting enzymes of triacylglycerol biosynthesis. Biochim Biophys Acta Mol Cell Biol Lipids 2009, 1791: 501−506
59. Grossmann ME, Nkhata KJ, Mizuno NK, Ray A, Cleary MP: Effects of adiponectin on breast cancer cell growth and signaling. Br J Cancer 2008, 98:370−379
60. Mociño-Rodríguez MD, Santillán-Benítez JG, Dozal-Domínguez DS, Hernández-Navarro MD, Flores-Merino MV, Sandoval-Cabrera A, García Vázquez FJ: Expression of AdipoR1 and AdipoR2 receptors as leptin-breast cancer regulation mechanisms. Dis Markers 2017, 2017:1−11
61. Andò S, Naimo GD, Gelsomino L, Catalano S, Mauro L: Novel insights into adiponectin action in breast cancer: evidence of its mechanistic effects mediated by ER[alpha] expression. Obes Rev 2020, 21:e13004
62. Ruiz M, Devkota R, Kaper D, Ruhanen H, Busayavalasa K, Radović U, Henricsson M, Käkelä R, Borén J, Pilon M: AdipoR2 recruits protein interactors to promote fatty acid elongation and membrane fluidity. J Biol Chem 2023, 299:104799
63. Yanai H, Yoshida H: Beneficial effects of adiponectin on glucose and lipid metabolism and atherosclerotic progression: mechanisms and perspectives. Int J Mol Sci 2019, 20:1190
64. Ntambi JM, Miyazaki M, Dobrzyn A: Regulation of stearoyl-CoA desaturase expression. Lipids 2004, 39:1061−1065
65. Griffiths B, Lewis CA, Bensaad K, Ros S, Zhang Q, Ferber EC, Konisti S, Peck B, Miess H, East P, Wakelam M, Harris AL, Schulze A: Sterol regulatory element binding protein-dependent regulation of lipid synthesis supports cell survival and tumor growth. Cancer Metab 2013, 1:3
66. Flowers MT, Ntambi JM: Role of stearoyl-coenzyme A desaturase in regulating lipid metabolism. Curr Opin Lipidol 2008, 19:248−256
67. Ranhotra HS: The estrogen-related receptors in metabolism and cancer: newer insights. J Receptors Signal Transduction Res 2018, 38:95−100
68. Huang W-Y, Sun P-M: Estrogen receptor-associated receptor [alpha] and peroxisome proliferator-activated receptor [gamma] in metabolism and disease (review). Mol Med Rep 2020, 23:156
69. Sadeghi MB, Nakhaee A, Saravani R, Sargazi S: Significant association of LXR[beta] (NR1H2) polymorphisms (rs28514894,

rs2303044) with type 2 diabetes mellitus and laboratory characteristics. J Diabetes Metab Disord 2021, 20:261−270
70. Kim M-Y, Koh D-I, Choi W-I, Jeon B-N, Jeong D, Kim K-S, Kim K, Kim S-H, Hur M-W: ZBTB2 increases PDK4 expression by transcriptional repression of RelA/p65. Nucleic Acids Res 2015, 43: 1609−1625
71. Jiang J, Wang S, Li Y, Wang Y, Liao R: Has-miR-199a-3p/RELA/SCD inhibits immune checkpoints in AMD and promotes macrophage-mediated inflammation and pathological angiogenesis through lipid metabolism pathway: a computational analysis. PLoS One 2024, 19:e0297849
72. Yao W, Wang T, Huang F: p300/CBP as a key nutritional sensor for hepatic energy homeostasis and liver fibrosis. Biomed Res Int 2018, 2018:1−14
73. Huang H, Tang S, Ji M, Tang Z, Shimada M, Liu X, Qi S, Locasale JW, Roeder RG, Zhao Y, Li X: p300-Mediated lysine 2-hydroxyisobutyrylation regulates glycolysis. Mol Cell 2018, 70: 663−678.e6
74. Lin J, Xia L, Oyang L, Liang J, Tan S, Wu N, Yi P, Pan Q, Rao S, Han Y, Tang Y, Su M, Luo X, Yang Y, Chen X, Yang L, Zhou Y, Liao Q: The POU2F1-ALDOA axis promotes the proliferation and chemoresistance of colon cancer cells by enhancing glycolysis and the pentose phosphate pathway activity. Oncogene 2022, 41: 1024−1039
75. Huang W-L, Abudureheman T, Xia J, Chu L, Zhou H, Zheng W-W, Zhou N, Shi R-Y, Li M-H, Zhu J-M, Qing K, Ji C, Liang K-W, Guo S, Yin G, Duan C-W: CDK9 inhibitor induces the apoptosis of B-cell acute lymphocytic leukemia by inhibiting c-Myc-mediated glycolytic metabolism. Front Cell Dev Biol 2021, 9:641271
76. Yuan X-N, Shao Y-C, Guan X-Q, Liu Q, Chu M-F, Yang Z-L, Li H, Zhao S, Tian Y-H, Zhang J-W, Wei L: METTL3 orchestrates glycolysis by stabilizing the c-Myc/WDR5 complex in triple-negative breast cancer. Biochim Biophys Acta Mol Cell Res 2024, 1871:119716
77. Li B, Wen M, Gao F, Wang Y, Wei G, Duan Y: Regulation of HNRNP family by post-translational modifications in cancer. Cell Death Discov 2024, 10:427
78. Clower CV, Chatterjee D, Wang Z, Cantley LC, Vander Heiden MG, Krainer AR: The alternative splicing repressors hnRNP A1/A2 and PTB influence pyruvate kinase isoform expression and cell metabolism. Proc Natl Acad Sci U S A 2010, 107:1894−1899
79. Shen Y, Wang Y, Zhang Y, Ma S, Yang L, Zhao C, Huang X: Targeting cyclin-dependent kinase 9 in cancer therapy. Acta Pharmacol Sin 2022, 43:1633−1645
80. Itkonen HM, Poulose N, Walker S, Mills IG: CDK9 Inhibition induces a metabolic switch that renders prostate cancer cells dependent on fatty acid oxidation. Neoplasia 2019, 21:713−720
81. Hussein S, Khanna P, Yunus N, Gatza ML: Nuclear receptor-mediated metabolic reprogramming and the impact on HR+ breast cancer. Cancers (Basel) 2021, 13:4808
82. Nowińska K, Jabłońska K, Ciesielska U, Piotrowska A, Haczkiewicz-Leśniak K, Pawełczyk K, Podhorska-Okołów M, Dzięgiel P: Association of irisin/FNDC5 with ERR[alpha] and PGC-1[alpha] expression in NSCLC. Int J Mol Sci 2022, 23:14204
83. Vergani E, Beretta GL, Aloisi M, Costantino M, Corno C, Frigerio S, Tinelli S, Dugo M, Accattatis FM, Granata A, Arnaboldi L, Rodolfo M, Perego P, Gatti L: Targeting of the lipid metabolism impairs resistance to BRAF kinase inhibitor in melanoma. Front Cell Dev Biol 2022, 10:927118
84. Scott JS, Nassar ZD, Swinnen JV, Butler LM: Monounsaturated fatty acids: key regulators of cell viability and intracellular signaling in cancer. Mol Cancer Res 2022, 20:1354−1364
85. Sun Q, Xing X, Wang H, Wan K, Fan R, Liu C, Wang Y, Wu W, Wang Y, Wang R: SCD1 is the critical signaling hub to mediate metabolic diseases: mechanism and the development of its inhibitors. Biomed Pharmacother 2024, 170:115586
86. García-Miranda A, Montes-Alvarado JB, Sarmiento-Salinas FL, Vallejo-Ruiz V, Castañeda-Saucedo E, Navarro-Tito N, Maycotte P: Regulation of mitochondrial metabolism by autophagy supports leptin-induced cell migration. Sci Rep 2024, 14:1408
87. Blanquer-Rosselló MM, Oliver J, Sastre-Serra J, Valle A, Roca P: Leptin regulates energy metabolism in MCF-7 breast cancer cells. Int J Biochem Cell Biol 2016, 72:18−26
88. Pham D, Tilija Pun N, Park P: Autophagy activation and SREBP-1 induction contribute to fatty acid metabolic reprogramming by leptin in breast cancer cells. Mol Oncol 2021, 15:657−678
89. Gelsomino L, Barone I, Caruso A, Giordano F, Brindisi M, Morello G, Accattatis FM, Panza S, Cappello AR, Bonofiglio D, Andò S, Catalano S, Giordano C: Proteomic profiling of extracellular vesicles released by leptin-treated breast cancer cells: a potential role in cancer metabolism. Int J Mol Sci 2022, 23:12941
90. Vander Heiden MG, Cantley LC, Thompson CB: Understanding the Warburg effect: the metabolic requirements of cell proliferation. Science 2009, 324:1029−1033
91. Ray A, Cleary MP: The potential role of leptin in tumor invasion and metastasis. Cytokine Growth Factor Rev 2017, 38:80−97
92. Fiorillo M, Lamb R, Tanowitz HB, Cappello AR, Martinez-Outschoorn UE, Sotgia F, Lisanti MP: Bedaquiline, an FDA-approved antibiotic, inhibits mitochondrial function and potently blocks the proliferative expansion of stem-like cancer cells (CSCs). Aging 2016, 8:1593−1607
93. Fiorillo M, Scatena C, Naccarato AG, Sotgia F, Lisanti MP: Bedaquiline, an FDA-approved drug, inhibits mitochondrial ATP production and metastasis in vivo, by targeting the gamma subunit (ATP5F1C) of the ATP synthase. Cell Death Differ 2021, 28:2797−2817
94. Chaudhary S, Shah A, Pothuraju R, Lakshmanan I, Ganti AK, Batra SK: Cancer metabolism and aggressive tumor behavior, Immuno-Oncology Crosstalk and Metabolism. Singapore, Springer Nature Singapore, 2022. pp. 21−43
95. Sudan SK, Sharma A, Vikramdeo KS, Davis W, Deshmukh SK, Poosarla T, Holliday NP, Prodduturvar P, Nelson C, Singh KP, Singh AP, Singh S: Obesity and early-onset breast cancer and specific molecular subtype diagnosis in black and white women. JAMA Netw Open 2024, 7:e2421846
96. Tong Y, Zhu S, Chen W, Chen X, Shen K: Association of obesity and luminal subtypes in prognosis and adjuvant endocrine treatment effectiveness prediction in Chinese breast cancer patients. Front Oncol 2022, 12:862224
97. Guo S, Wang Y, Zhou D, Li Z: Significantly increased monounsaturated lipids relative to polyunsaturated lipids in six types of cancer microenvironment are observed by mass spectrometry imaging. Sci Rep 2014, 4:5959
98. Roongta UV, Pabalan JG, Wang X, Ryseck R-P, Fargnoli J, Henley BJ, Yang W-P, Zhu J, Madireddi MT, Lawrence RM, Wong TW, Rupnow BA: Cancer cell dependence on unsaturated fatty acids implicates stearoyl-CoA desaturase as a target for cancer therapy. Mol Cancer Res 2011, 9:1551−1561
99. von Roemeling CA, Marlow LA, Wei JJ, Cooper SJ, Caulfield TR, Wu K, Tan WW, Tun HW, Copland JA: Stearoyl-CoA desaturase 1 is a novel molecular therapeutic target for clear cell renal cell carcinoma. Clin Cancer Res 2013, 19:2368−2380
100. Li W, Bai H, Liu S, Cao D, Wu H, Shen K, Tai Y, Yang J: Targeting stearoyl-CoA desaturase 1 to repress endometrial cancer progression. Oncotarget 2018, 9:12064−12078
101. Piao C, Cui X, Zhan B, Li J, Li Z, Li Z, Liu X, Bi J, Zhang Z, Kong C: Inhibition of stearoyl CoA desaturase-1 activity suppresses tumour progression and improves prognosis in human bladder cancer. J Cell Mol Med 2019, 23:2064−2076
102. von Roemeling CA, Marlow LA, Pinkerton AB, Crist A, Miller J, Tun HW, Smallridge RC, Copland JA: Aberrant lipid metabolism in anaplastic thyroid carcinoma reveals stearoyl CoA desaturase 1 as a novel therapeutic target. J Clin Endocrinol Metab 2015, 100: E697−E709

103. Scaglia N, Chisholm JW, Igal RA: Inhibition of stearoylCoA desaturase-1 inactivates acetyl-CoA carboxylase and impairs proliferation in cancer cells: role of AMPK. PLoS One 2009, 4: e6812
104. Mauvoisin D, Charfi C, Lounis AM, Rassart E, Mounier C: Decreasing stearoyl-CoA desaturase-1 expression inhibits [beta]-catenin signaling in breast cancer cells. Cancer Sci 2013, 104: 36−42
105. Angelucci C, D'Alessio A, Iacopino F, Proietti G, Di Leone A, Masetti R, Sica G: Pivotal role of human stearoyl-CoA desaturases (SCD1 and 5) in breast cancer progression: oleic acid-based effect of SCD1 on cell migration and a novel pro-cell survival role for SCD5. Oncotarget 2018, 9:24364−24380
106. Angelucci C, Maulucci G, Colabianchi A, Iacopino F, D'Alessio A, Maiorana A, Palmieri V, Papi M, De Spirito M, Di Leone A, Masetti R, Sica G: Stearoyl-CoA desaturase 1 and paracrine diffusible signals have a major role in the promotion of breast cancer cell migration induced by cancer-associated fibroblasts. Br J Cancer 2015, 112:1675−1686
107. Samuel W, Nagineni CN, Kutty RK, Parks WT, Gordon JS, Prouty SM, Hooks JJ, Wiggert B: Transforming growth factor-[beta] regulates stearoyl coenzyme A desaturase expression through a Smad signaling pathway. J Biol Chem 2002, 277:59−66
108. Demoulin J-B, Ericsson J, Kallin A, Rorsman C, Rönnstrand L, Heldin C-H: Platelet-derived growth factor stimulates membrane lipid synthesis through activation of phosphatidylinositol 3-kinase and sterol regulatory element-binding proteins. J Biol Chem 2004, 279:35392−35402
109. Olichwier A, Balatskyi VV, Wolosiewicz M, Ntambi JM, Dobrzyn P: Interplay between thyroid hormones and stearoyl-CoA desaturase 1 in the regulation of lipid metabolism in the heart. Int J Mol Sci 2020, 22:109
110. Mauvoisin D, Rocque G, Arfa O, Radenne A, Boissier P, Mounier C: Role of the PI3-kinase/mTor pathway in the regulation of the stearoyl CoA desaturase (SCD1) gene expression by insulin in liver. J Cell Commun Signal 2007, 1:113−125
111. Mauvoisin D, Mounier C: Hormonal and nutritional regulation of SCD1 gene expression. Biochimie 2011, 93:78−86
112. Nagarajan SR, Butler LM, Hoy AJ: The diversity and breadth of cancer cell fatty acid metabolism. Cancer Metab 2021, 9:2
113. Currie E, Schulze A, Zechner R, Walther TC, Farese RV: Cellular fatty acid metabolism and cancer. Cell Metab 2013, 18:153−161
114. Cheng S, Zhang D, Feng J, Hu Q, Tan A, Xie Z, Chen Q, Huang H, Wei Y, Ouyang Z, Ma X: Metabolic pathway of monounsaturated lipids revealed by in-depth structural lipidomics by mass spectrometry. Research (Wash D C) 2023, 6:0087
115. Guo Z, Bergeron K-F, Lingrand M, Mounier C: Unveiling the MUFA−cancer connection: insights from endogenous and exogenous perspectives. Int J Mol Sci 2023, 24:9921
116. Gangl A, Kornauth W, Mlczoch J, Sulm O, Klose B: Different metabolism of saturated and unsaturated long chain plasma free fatty acids by intestinal mucosa of rats. Lipids 1980, 15:75−79
117. Feingold KR: Obesity and dyslipidemia. In: Feingold KR, Ahmed SF, Anawalt B, Blackman MR, Boyce A, Chrousos G, Corpas E, de Herder WW, Dhatariya K, Dungan K, Hofland J, Kalra S, Kaltsas G, Kapoor N, Koch C, Kopp P, Korbonits M, Kovacs CS, Kuohung W, Laferrère B, Levy M, McGee EA, McLachlan R, Muzumdar R, Purnell J, Rey R, Sahay R, Shah AS, Singer F, Sperling MA, Stratakis CA, Trence DL, Wilson DP, editors. Endotext [Internet]. South Dartmouth, MA: MDText.com, Inc., 2000. Available at: https://www.ncbi.nlm.nih.gov/books/NBK305895 (last update June 19, 2023)
118. Park J, Kusminski CM, Chua SC, Scherer PE: Leptin receptor signaling supports cancer cell metabolism through suppression of mitochondrial respiration in vivo. Am J Pathol 2010, 177: 3133−3144
119. Reidy SP, Weber J-M: Leptin: an essential regulator of lipid metabolism. Comp Biochem Physiol A Mol Integr Physiol 2000, 125:285−298
120. Harris RBS: Direct and indirect effects of leptin on adipocyte metabolism. Biochim Biophys Acta 2014, 1842:414−423
121. Goodwin PJ, Chen BE, Gelmon KA, Whelan TJ, Ennis M, Lemieux J, Ligibel JA, Hershman DL, Mayer IA, Hobday TJ, Bliss JM, Rastogi P, Rabaglio-Poretti M, Mukherjee SD, Mackey JR, Abramson VG, Oja C, Wesolowski R, Thompson AM, Rea DW, Stos PM, Shepherd LE, Stambolic V, Parulekar WR: Effect of metformin vs placebo on invasive disease−free survival in patients with breast cancer. JAMA 2022, 327:1963
122. Bridges HR, Blaza JN, Yin Z, Chung I, Pollak MN, Hirst J: Structural basis of mammalian respiratory complex I inhibition by medicinal biguanides. Science 2023, 379:351−357
123. Stevens AM, Xiang M, Heppler LN, Tošić I, Jiang K, Munoz JO, Gaikwad AS, Horton TM, Long X, Narayanan P, Seashore EL, Terrell MC, Rashid R, Krueger MJ, Mangubat-Medina AE, Ball ZT, Sumazin P, Walker SR, Hamada Y, Oyadomari S, Redell MS, Frank DA: Atovaquone is active against AML by upregulating the integrated stress pathway and suppressing oxidative phosphorylation. Blood Adv 2019, 3:4215−4227
124. Fiorillo M, Lamb R, Tanowitz HB, Mutti L, Krstic-Demonacos M, Cappello AR, Martinez-Outschoorn UE, Sotgia F, Lisanti MP: Repurposing atovaquone: targeting mitochondrial complex III and OXPHOS to eradicate cancer stem cells. Oncotarget 2016, 7: 34084−34099